



**HAL**  
open science

## Geological probability of success assessment for amplitude-driven Prospects: A Nile Delta case study

Nicolas Nosjean, R. Holeywell, H.S. Pettingill, R. Roden, M. Forrest

### ► To cite this version:

Nicolas Nosjean, R. Holeywell, H.S. Pettingill, R. Roden, M. Forrest. Geological probability of success assessment for amplitude-driven Prospects: A Nile Delta case study. *Journal of Petroleum Science and Engineering*, 2021, 202, pp.108515. 10.1016/j.petrol.2021.108515 . hal-04504103

**HAL Id: hal-04504103**

**<https://hal.science/hal-04504103>**

Submitted on 22 Jul 2024

**HAL** is a multi-disciplinary open access archive for the deposit and dissemination of scientific research documents, whether they are published or not. The documents may come from teaching and research institutions in France or abroad, or from public or private research centers.

L'archive ouverte pluridisciplinaire **HAL**, est destinée au dépôt et à la diffusion de documents scientifiques de niveau recherche, publiés ou non, émanant des établissements d'enseignement et de recherche français ou étrangers, des laboratoires publics ou privés.



Distributed under a Creative Commons Attribution - NonCommercial 4.0 International License

# Geological Probability Of Success Assessment for Amplitude-Driven Prospects: A Nile Delta Case Study.

N. Nosjean <sup>a</sup>, R. Holeywell <sup>b</sup>, H. S. Pettingill <sup>b</sup>, R. Roden <sup>c</sup>, M. Forrest <sup>d</sup>

<sup>a</sup> Paris-Saclay university, CNRS, GEOPS, 91405, Orsay, France

<sup>b</sup> Rose & Associates., 1334 Brittmoore Road, Ste. 2801 Houston, Texas, 77043, USA

<sup>c</sup> Rocky Ridge Resources, Inc. 4927 CR 2161 Centerville, Texas, 75833, USA

<sup>d</sup> Consultant, Dallas Texas

---

## Abstract

Effective quantification and management of exploration risks and associated uncertainties remains a key challenge for the Oil and Gas industry. Geological probability of success evaluation is one of the key steps of the exploration process, which will lead - if properly managed - to enhanced project's value creation, as well as improved portfolio management and exploration decisions. This paper reviews and discusses a consistent, uniform and reproducible approach for evaluating seismic amplitude-supported prospects, weighted by the input data quality and availability. The method and workflows are further illustrated with an offshore Nile Delta case study. This approach enhances the confidence in the appropriate risk and associated resource estimate for less biased and more consistent probability estimation.

*Keywords: risk analysis, probability of success, portfolio management, uncertainty, subsurface geology, geophysics, seismic amplitudes, seismic attributes, DHI, DHI uplift, hydrocarbon exploration, bias mitigation, seismic interpretation, petroleum system elements, Pliocene, Nile Delta, Egypt.*

---

## Introduction

The purpose of this article is to present a risk evaluation methodology aimed at delivering an efficient and systematic geological probability of success (Pg) analysis. This approach can be applied to the exploration portfolio of an Exploration and Production (E&P) company, to simplify drilling decisions and to provide a framework for consistent decision making under uncertainty. This paper focuses on conventional prospects characterized by seismic amplitude support (see definitions in part 3 of the present publication), common in gas fluid-type prospects (Westwood Group, 2019). After reviewing the main elements for geological and geophysical risk assessment, we will detail the proposed methodology using a case study located in the offshore Egyptian Nile Delta.

### 1. Prospect Risk Assessment Generalities

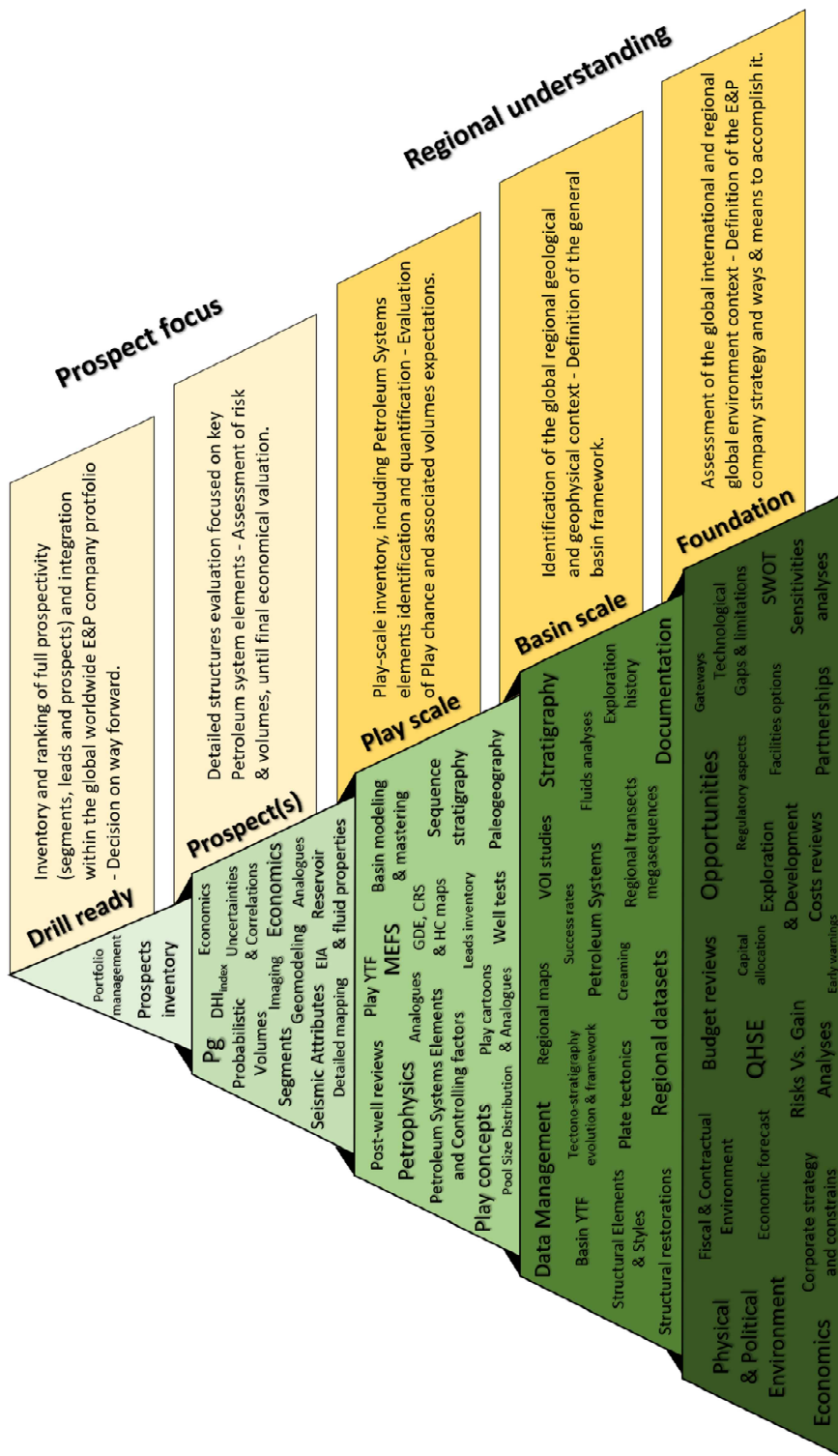
#### 1.1 Problematic & Definitions

Exploring for hydrocarbon (and especially gas) resources and bringing them into production requires an in-depth understanding of the geological context and its challenges. To account for the increasingly complex conditions (e.g. geological, environmental, political) and the associated risks and uncertainties in which this search takes place (Smalley et al., 2008; Citron et al., 2017), a large amount of data and associated relevant studies need to be performed at different scales. These range from regional basin analysis to prospect-scale detailed evaluations, as synthesized on **Figure 1**.

According to Rose (1992, 2001a), the probability of geological success (Pg) represents the chance of finding hydrocarbons in a reservoir capable of sustained flow. This value - expressed in percentage - is commonly used to rank segments and prospects by risked prospective resource calculations (White, 1993). It represents the first step of a series of investment decisions.

The evaluation of Pg is a key and challenging task that requires detailed and sequential analyses of all the various elements (called chance or risk factors in the literature) defining the Petroleum System at both play and prospect scales. To calculate the Pg value, most companies multiply a certain number of independent chance (or risk) factor elements representing the likelihood of each key Petroleum System parameter to be present (Milkov, 2015; Rose, 2001b; Gotautas, 1963).

Each E&P company typically defines its own chance factor elements, which can vary in number from four (Duff and Hall, 1996; Snow et al., 1996; Johns et al., 1998) to more than fifty (Watson, 1998). However, they are commonly grouped in five independent categories (see Rose, 2001b and Part 2 of this paper), which are: Source, Migration and Timing, Reservoir Rocks, Structure (i.e. Closure), and eventually Containment (i.e. Seal and Preservation).



Used abbreviations: Pg: geological probability; DHI: Direct Hydrocarbon Indicator; EIA: Environmental Impact Assessment; YTF: Yet To Find; GDE: Gross Depositional Environment; CRS: Common Reservoir Segment; HC: Hydrocarbon; QHSE: Quality Health, Safety and Environment; SWOT: Strength, Weakness, Opportunity and Threat.

**Figure 1: The Exploration triangle.**

(inspired from Fraser, 2011, Peel et al., 2015a, 2015b, Milkov, 2015, and Milkov and Samis, 2020).

Efficient and successful exploration requires evaluations of subsurface risk and uncertainty starting from the regional and play level, so that dependencies at prospect level can be quantified and understood. Such regional evaluations require efficient access to a comprehensive and high-quality well and seismic database on a basin-wide scale, incorporating lessons learned from both successes and failures. The analysis is refined on a step-by-step approach until a drill ready structure is defined. Acronym definitions: HC: Hydrocarbon; DHI: Direct Hydrocarbon Indicator; EIA: Environmental Impact Assessment; GDE: Gross Depositional Environment; CRS: Common Risk Segment; YTF: Yet To Find; VOI: Value Of Information; QHSE: Quality Health Security Environment; SWOT: Strength Weakness Opportunity Threat.

Even with an agreed methodology, this approach often leads to inconsistency in the Pg evaluation. This Pg estimation is often based on subjective judgments of the individual geological Petroleum System probability components and is subject to personal and group biases, heuristics and fallacies factors, such as base rate neglect (Milkov, 2017), cognitive and motivational biases (Merckhofer, 1987), anchoring bias (Tversky and Kahneman, 1974), expectation bias (Jeng, 2006), conservatism or optimism biases (Baron, 1997; Rose and Citron, 2000; Fischhoff et al., 1977), confirmation bias (Oswald and Grosjean, 2004) and many more (see Capen, 1976, Fischhoff et al., 1977, Merckhofer, 1987, Bárdossy, 2003, Baddeley et al., 2004, Citron et al., 2018 and Milkov, 2015).

In addition, as we will detail later in this paper, the presence of seismic amplitude anomalies within a given prospect, may also alter the interpreter's evaluation on the various risks factors if not evaluated independently. These personal and collective subjective biases may eventually produce inconsistent prospect portfolio evaluations across an E&P company, ultimately failing to deliver promised financial and operational goals.

### 1.2 General approach

In order to obtain a reliably ranked portfolio, each prospect or segment, and their associated Petroleum System elements, must be assessed independently but in a consistent manner (Rose and Citron, 2000).

To detect and limit the previously mentioned biases that can negatively alter exploration decisions, various

methods or best practices are routinely used. These include reality checks of estimated parameters, calibrated project evaluations, performance tracking (Rose, 2017), combination and integration of various technologies in the prospect assessment (e.g. microseepage, inversion, gravity and EM - Hesthammer et al., 2010; Schumacher, 2012; Maver, 2019a, 2019b), centralized quality assurance teams, decision making processes, value of information analyses, or more recently using database mining and artificial intelligence tools (Geng et al., 2019).

A common method to calculate Pg is based on an approach popularized in the E&P industry by Rose (1987, 1992, 2004). This is the chance adequacy matrix table, as illustrated in Figure 2. This concept is based on the fact that good quality data available for an evaluation will tend to lead to a Pg estimate of a Petroleum System element towards the positive or negative side (i.e. high or low risk factor success likelihood).

However, if the data available are limited, the estimates will tend to pool around the middle. This concept can be very powerful, as it establishes - thanks to Pg probabilities estimates - a direct linkage between the data quality and associated derived information (Kahneman and Tversky, 1979; Duff and Hall, 1996; Watson, 1998; CCOP, 2000; Fournier et al., 2013; Kunjan, 2016).

Nevertheless, its implementation is not a straightforward task (Sykes et al., 2011), this approach being still subject to expert judgment biases when selecting a box in the table or even an exact value within a given box.

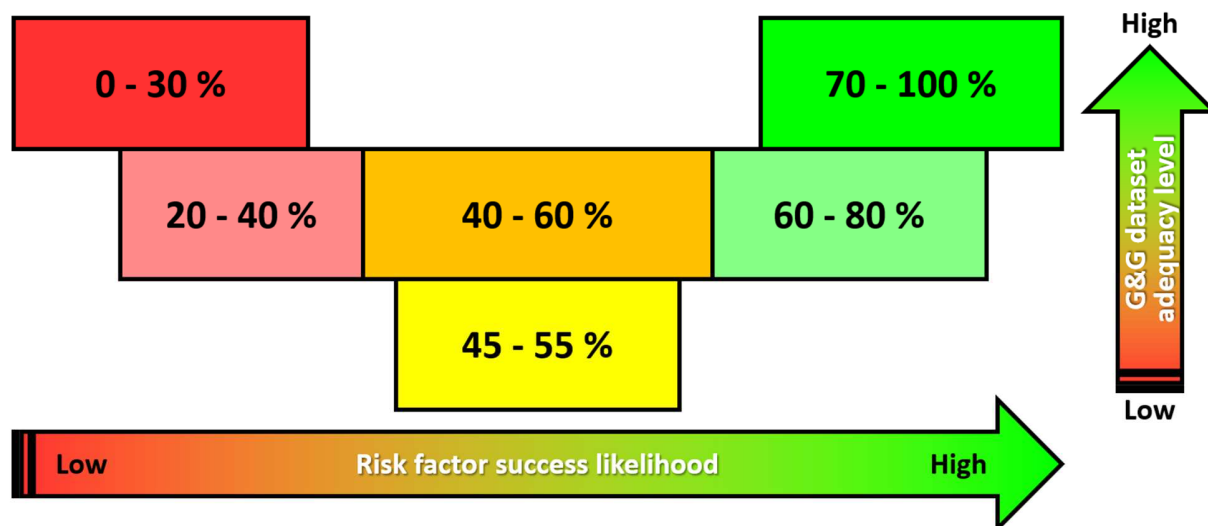


**Figure 2:** The chance adequacy matrix.  
(from Rose, 2001b, modified)

In the Chance-Adequacy matrix, the horizontal axis is the level of confidence (low or high) that the considered risk factor will be sufficient for a successful prospect outcome, i.e. will not be the cause of failure (Peel and Brooks, 2016). The vertical axis is the adequacy of the available Geological and Geophysical (G&G) data - in term of quantity, quality, and the number, pertinence and proximity of control points. Percentage values in the cells are representative of the success chances that might be assigned for that risk component. Key point is that if there is little data, assessments will often approach a 'coin-flip' (50-50), whereas the availability of more data commonly forces the assessment to be either more strongly positive or negative.

To avoid this issue and to improve objectivity, predictability and consistency in the risking process, the method proposed in this paper is based on the workflow developed by the Rose & Associates DHI Consortium (DHI stands for Direct Hydrocarbon Indicator, see definition later). It follows the Einstein suggestion to: “make things as simple as possible, but not simpler” (also refer to [Milkov \(2015\)](#) Alternative matrix approach).

The methodology developed by the consortium since its creation in 2000 follows a three-step process, as illustrated in **Figure 3**:

- 1- Calculation of the Initial Pg,
- 2- Calculation of the DHI Index,
- 3- Generation of the revised Pg.

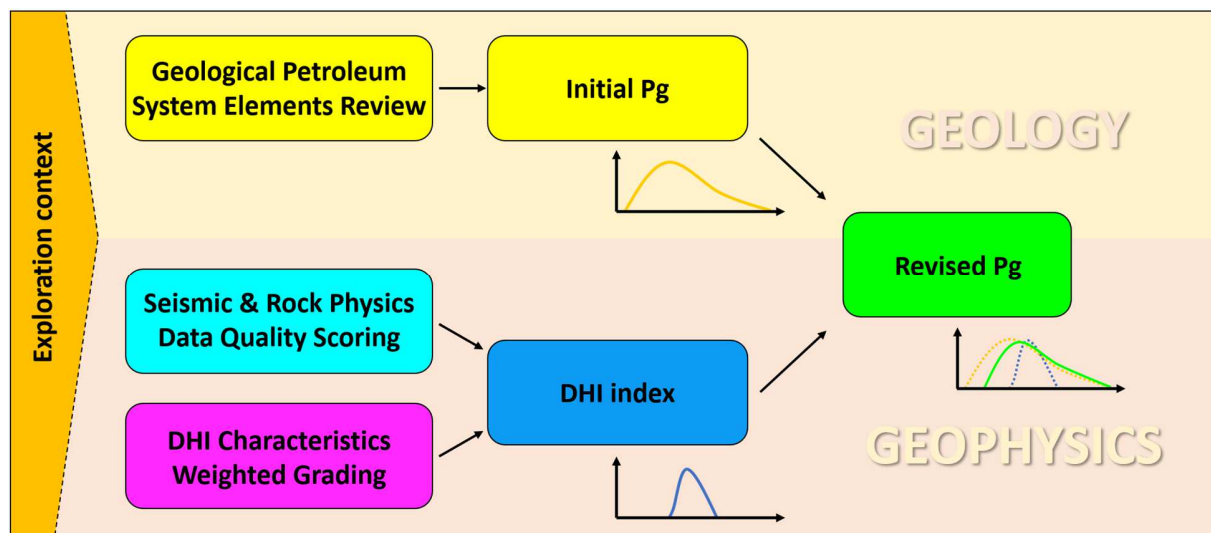


**Figure 3:** The risk factors assessment proposed workflow.

The figure presents the main steps of the Pg calculation for a given prospect using the workflow developed by the DHI Consortium. The Exploration context is referring to all key studies needed to be performed prior to the detailed prospect analysis, as described on the first three bottom layers of the Exploration triangle in **Figure 1**.

The Initial Pg is first calculated based on a detailed review of the geological elements within the studied petroleum system play. If we are in the presence of a seismic amplitude supported prospect, the Pg can be modified using a DHI Index based on a review and scoring procedure combining both data quality and DHI characteristics evaluation. The revised Pg can then be obtained by the combination of the Initial Pg weighted by the DHI Index.

The Initial Pg assessment is based on regional and local geological interpretation using information such as structural maps, depositional models, basin modeling results, well derived information... (see **Figure 1**).

By definition, Initial Pg ignores all the associated information resulting from the interpretation of seismic amplitude anomalies perceived to be Direct Hydrocarbon Indicators (DHIs). For example, a stratigraphic prospect purely defined on a seismic amplitude anomaly will have an extremely low Initial Pg, as the assessment of the petroleum system elements based only on geological information will not be easily identifiable.

The Initial Pg value should be set in a very consistent and rigorous manner among all prospects and segments within a given E&P company portfolio, as it constitutes a key anchor point for a reliable evaluation of a given prospect ([Roden et al., 2005](#)). This value will be the starting point of the DHI evaluation process.

The DHI Index calculated in the next step will only modify positively or negatively this Initial Pg value ([Sansal, 2014](#)). As we will detail later, the DHI Index will be the result of the DHI characteristics grading, weighted by a data quality scoring factor. It will then be possible to derive the revised Pg.

The goal is to deliver an objective and consistent prospect evaluation based on subsurface data and related interpretation from both a geological and geophysical (G&G) point of view ([Laver et al., 2012](#)).

This method provides more than a simple risk assessment guideline, but a complete evaluation tool incorporating all the foundations of petroleum system principles. It converts G&G interpretations into reliable and robust quantitative probabilities.

We will now detail the three steps of the Pg assessment procedure.

## 2. Initial Pg assessment procedure

The risk assessment of a given prospect or segment consists initially of estimating the probability of geological success, considering the random factors of all the elements of the Petroleum System being independent from the seismic information related to the fluid effects. In other words, all the geologic risk factors considered in the estimation of the Initial Pg are estimated without considering seismic amplitude anomalies as direct hydrocarbon indicators.

One of the traditional approaches to Pg assessment is based on the work of [Rose \(2004\)](#) and is comprised of five categories of independent random geological factors:

- 1) **The probability of the presence and quality of the source rock.** It must be thermally mature and be present in sufficient volume. It must have a richness (from an organic point of view, i.e. TOC), a thickness, and enough extent to be able to generate volumes of hydrocarbons allowing at least the minimum filling case of the evaluated prospect.
- 2) **The probability of an effective migration pathway leading to closures that existed at the time of migration.** This hydrocarbon migration must be efficient enough to charge the closures with volumes adequate to detect.
- 3) **The probability of the presence and quality of reservoir rock from the time of migration until today** (e.g. with limited diagenetic effects, erosion). The reservoir must be at least of some minimal thickness sufficient to contain detectable quantities of hydrocarbons.
- 4) **The probability of the presence and effectiveness of a closure (i.e. being able to retain HC) in the assessed prospect.** These include structural or stratigraphic traps and the confidence that the traps have been mapped accurately.
- 5) **The probability of containment of the evaluated closure.** This relates to the presence of adequate sealing rocks able to retain the HC at least for the minimum estimated volume case. The containment must preserve through time the accumulated HC from any leakage, flushing or degradation.

The key elements and processes of the Petroleum System evaluated for the calculation of the Initial Pg are summarized on [Figure 4](#). The key point in assessing these primary geological risk factors is that each of them is of equal importance. In the event of failure of only one of them, there will be no HC trapped within the evaluated prospect.

Geoscientists often estimate these five geologic chance factors using expert knowledge and experience. From an operational and practical point of view, the DHI Consortium has developed an alternative Initial Pg

procedure that helps geoscientists assess the geologic chance factors by systematically answering a specific set of questions that are the most relevant for each chance factor element. Following the given responses, the initial Pg is then calculated for each risk factor with a matrix combination of data quality evaluation (from left to right) and favorability assessment (from top to bottom), as detailed in [Figure 5](#). During this Initial Pg assessment procedure, interpreters must answer up to 25 key qualitative inquiries.

This method has many advantages, notably it can be used as a consistent, systematic and auditable checklist, enabling the identification of critical risk factors in an assessed prospect. Thereby, G&G teams can generate dedicated studies or additional analyses relatively early in the exploration process in order to derisk each component of the Petroleum System.

This Initial Pg procedure enables:

- Interpreters to gather and assess systematically, and at the same evaluation level, all the Petroleum System geological factors.
- The immediate identification of the weak evaluation points or gaps of the studied prospect, from the point of view of either study element information or data availability.
- A transparent evaluation process that is easily controllable by a team of experts. As such, during peer-reviews, the discussions can be pointed directly on G&G interpretation issues and associated geological model expectations, rather than spending time to agree on an exact Pg risk factor value.
- Removal of subjectivity in the selection of a given cell in the risk table thanks to replying to systematic questions rather than using a common risk table.
- Less dependency on the experience or personal preferences of each assessor (notably motivational bias, [Merckhofer, 1987](#), and overconfidence bias, [Kahneman and Tversky, 1979](#); [Rose, 2001a, 2001b](#)). This is what [Milkov \(2015\)](#) defines as the difference between an expert judgment versus an algorithm.
- The final Pg to be less influenced by recent results (recent bias, [Milkov, 2015](#); [Syed, 2015](#)) or memorable analogues.
- The geoscientist to engage early in the evaluation process with a discussion of specific observations of a particular element of the Petroleum System for fine-tuning purposes ([Longley and Brown, 2016](#)).
- More consistency in the assessment of all prospects and associated segments ([Rose and Citron, 2000](#)), thereby improving the asset portfolio evaluation. This enables a

more accurate selection of the appropriate plays and prospects for the best investment decisions.

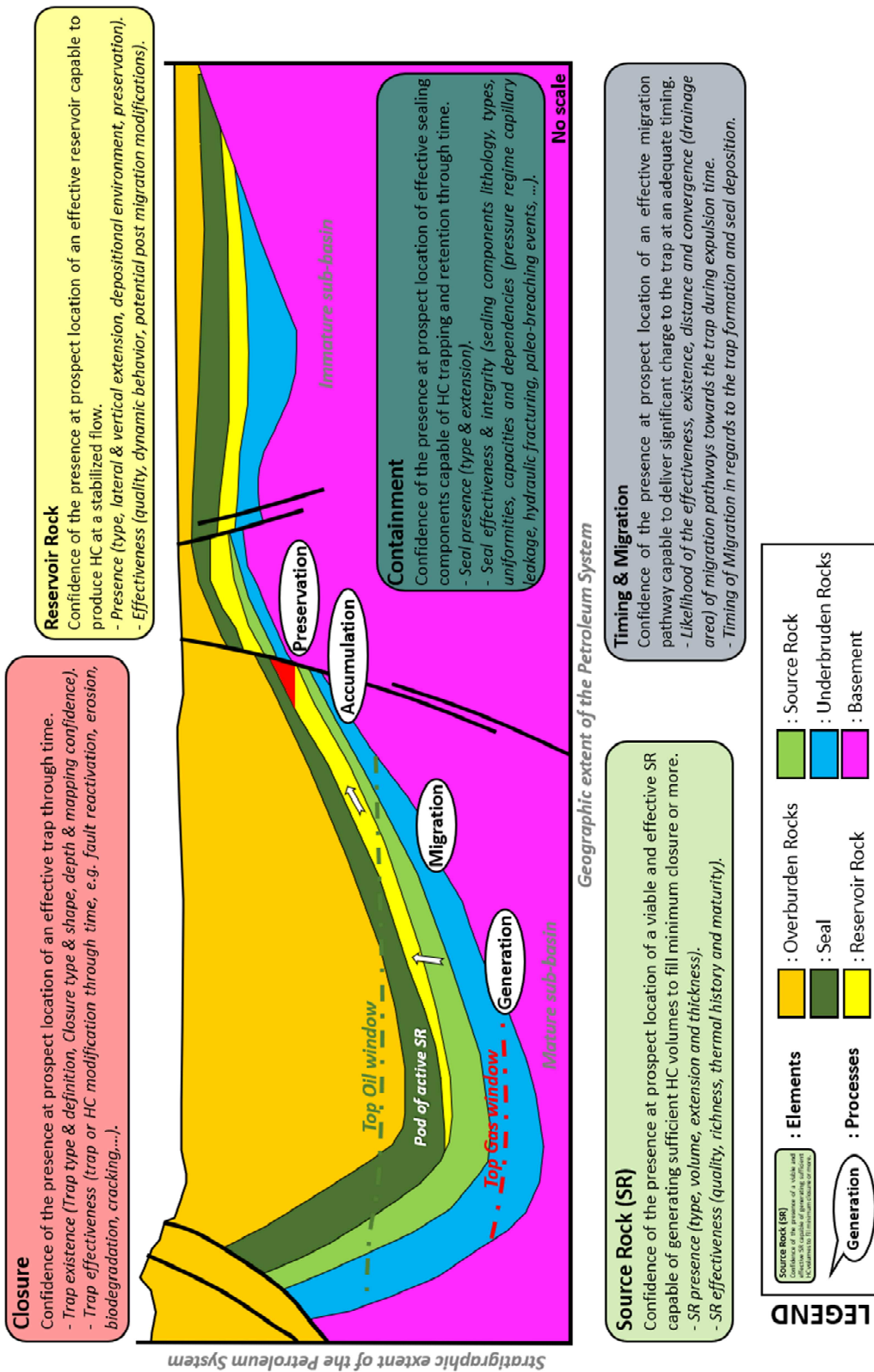


**Figure 4: Key Petroleum System elements and associated processes**

(inspired from Magoon, 1988, Magoon and Dow, 1994, Demaison and Huizinga, 1994 and Rose, 2001b).

A Petroleum System is defined as a set of five key elements (Source Rock, Timing and Migration, Reservoir Rock, Containment and Closure) and four key processes (Generation, Migration, Accumulation and Preservation) leading - if all present - to a hydrocarbon accumulation.



		Data Quality Score				
		High 5	4	3	2	Low 1
Assessment Score (based on observations)	<b>Reservoir Presence</b>					
	5) Proven. Regardless of depositional environment, multiple nearby wells show presence of clastic reservoir in the target formation, for the same depositional environment and depth range.	100	96	NP	NP	NP
	4) Well control establishes reservoir system, which can be reliably extended to the prospect location. Target is usually a laterally extensive clastic reservoir facies, such as shallow water marine sands deposited over large portions of the basin.	90	80	70	NP	NP
	3) High quality seismic stratigraphy without well control indicates presence of a laterally extensive reservoir. May also include limited extent reservoirs in a highly calibrated exploration play.	80	75	65	55	55
	2) Non-proven but well-understood models that project the presence of smaller, isolated deposits, such as alluvial fans, meandering channels, braided streams, or submarine fans.	70	55	50	50	45
1) Non-proven models that project the presence of highly restricted clastic reservoirs, such as narrow stream channels or small-scale lacustrine features. Would also apply to reservoir models that are atypical for the play.	60	55	50	40	40	

**Figure 5: Cross-reference table example supporting the query-based Initial Pg process for the probability of presence for a clastic reservoir.**

This table is conceptually similar to the Chance-Adequacy Matrix shown in Figure 2, except that the axes have been swapped for improved legibility. Cells labeled 'NP' are choices that are not allowed because it is logically inconsistent to assert a proven or near-proven Assessment score (4 or 5) and at the same time only a Low or Mid-range Data Quality score (1, 2, or 3). Red arrows show an example in which Reservoir Presence has been assessed at 2 and Data Quality at 3, producing an element chance of 50%.

Probability values within the risk tables such as presented on Figure 5 are based on specific geological information. As with the DHI assessment, grade descriptions and risk values initially represent a consensus of members' expert judgement but are improved over time as prospects are added to the Consortium's calibration library.

In these tables Data Quality is organized from left to right by columns, ranging from grade 5) being high-quality data, to grade 1) being very poor-quality data. The Data Quality grades are determined by the assessor's responses to specific questions related to the general exploration setting, structural control, well control, play and prospect maturity. Geological factor Assessment Scores are organized vertically into rows ranging also from grade 5) proven, to grade 1) non-proven. In general, grades 1) and 2) lead to a depreciation of the studied element, grade 3) is neutral, and grades 4) and 5) lead to an appreciation of the studied element.

As previously mentioned, this tool does not request a numeric chance input, but asks the assessor to compare the prospect against detailed and specific descriptions in order to arrive at a reliable grade. In the Figure 5 example, the assessor selected a grade of 3 for the Data Quality and a grade of 2 for the Assessment Score for the presence of a reservoir. At the intersection of the selected row and column, the probability factor result is 50%.

This value will be used in the calculation of the Initial Pg for this specific petroleum system element. We will repeat this exercise for all the risk factor elements in order to

calculate the Initial Pg value that will be used at the end of the process in combination with the DHI Index.

### 3. Amplitude-driven prospects - risk assessment and calculation of the DHI Index

It is commonly acknowledged that the presence of an amplitude anomaly in a given segment or prospect may have a significant influence on the risking of the individual geologic chance factors (Forrest et al., 2010; Roden et al., 2005). The challenge is to efficiently assess the confidence that a seismic amplitude anomaly is truly generated from the presence of hydrocarbon. This evaluation cannot be done until the relevant geophysical and associated geological subsurface data are collected and interpreted, models built and calibrated. In this paper the assessment of the DHI Index, which is a calculation of the interpreter's confidence that the amplitude anomaly is truly a DHI, has been developed by the DHI Consortium in a software application named SAAM (Seismic Amplitude Analysis Module).

The impact of seismic amplitude support on exploration performance has proven to be key, especially in the recent decade for stratigraphic and combined stratigraphic-structural traps. Fahmy and Reilly (2006) report a 20% increase in success rate using the seismic amplitude-driven technology. Westwood Group (2019, 2020) highlights a similar increase (15%) for technical discoveries in a 12 years period (2008-2019) on frontier DHI supported prospects, but the difference is less evident for mature plays (see also Rudolph and Goulding, 2017, Finlayson, 2018 and Pettingill et al., 2019 evaluations).

Before going into more details, it is important to understand key terms related to DHI evaluations:

- A **seismic amplitude anomaly** is a seismic event where the amplitude value differs from the background due to the acoustic impedance contrast (velocity x density) of the anomaly and the encasing rocks. This can be due to various reasons, such as lithology contrasts, geophysical artifacts, changes in reservoir properties, but also by the presence of compressible fluids.

- A **Direct Hydrocarbon Indicator (DHI)** is an amplitude anomaly that is specifically caused by the presence of hydrocarbons. Most DHIs are associated with an amplitude anomaly at its observed location, but they can also be found in the overlying sediment column (gas chimneys) or below the anomaly (shadow zones and velocity sags). Typical DHI characteristics are bright-spots, flat-spots, dim-spots, amplitude conformance to structure, polarity reversal, downdip-phase change, and the appropriate AVO response for the presence of hydrocarbons (see more on **Figure 7**).

In the evaluation process of interpreting DHIs, potential pitfalls must be considered where the seismic amplitude anomaly may have been generated by factors other than the presence of HC. These pitfalls produce a situation where the seismic amplitude anomaly can lead to a wrong interpretation. For example, an anomaly may have been interpreted as a flat-spot, indicative of a HC contact, when in reality it was the edge of a channel that was subsequently uplifted and exhibited a flat event.

To provide an efficient seismic amplitude and DHI evaluation - as we did for the Initial Pg evaluation - the input data quality needs first to be properly assessed, followed by a detailed analysis of the interpreted and calibrated models supporting both the observed seismic amplitude anomaly and the associated DHI observations.

Unlike the Petroleum System geological elements, the seismic amplitude DHI characteristics are not independent variables. Many DHI characteristics in a given prospect show different aspects of the same seismic anomaly and its relationships with the neighboring area, directly linked to the interpreted geological model. For example, amplitude conformance, seismic phase or character change, and tuning ring near the downdip edge of an anomaly are three distinct DHI characteristics displaying the transition from the hydrocarbon to the water leg (see examples given in [Ffrench, 2020a, b, c](#) and [Needham et al., 2017](#)).

Due to these clear dependencies, it is not possible, from a mathematical point of view, to multiply these various characteristics to obtain a "Pg DHI" that can be later combined with an Initial Pg. The chosen solution is to compute a "DHI Index", which will relate to the numerous DHI characteristic observations.

The methodology developed in the DHI Consortium allows an evaluation of seismic amplitude anomalies in a global and effective manner, without biasing the evaluation of

the geological chance factors. Indeed, as explained previously, to have a real DHI present on the seismic data, all the geological chance factors that constitutes the Petroleum System must work (i.e. 100% chance). The only exception to this rule is the presence of Low Saturation Gas (LSG), which can produce seismic DHI characteristics similar to that of commercial gas quantities ([Perveiz et al., 2010](#); [Rodén et al., 2014](#); [O'Brien, 2004, 2005](#); [Fahmy and Reilly, 2006](#); [Khalid et al., 2010](#)). The presence of thermogenic and/or microbial LSG with DHI support in a given reservoir generally indicates that a trapping configuration was present in the past, but where the closure was broken at some point, leading to HC leakage and leaving behind residual gas trapped by capillary pressures ([Holtz, 2002](#)). This is the well-known limitation of the use of seismic data and especially AVO information. We will now review the methodology implementing seismic amplitude anomalies and DHI characteristics that will eventually lead to the revision of the Initial Pg.

### 3.1. Data quality index computation

In order to correctly estimate the impact of the seismic amplitudes on the modification of the Initial Pg, it is necessary to first assess the quality, the quantity (including coverage) and the relevance of the seismic data, as well as the petroelastic information and associated models performed to support the interpretation. It should be noted that several sets of seismic data are often used during the interpretation. It is assumed that the highest quality dataset is used to make the final interpretations.

For data quality assessment, key questions are asked of the assessor such as:

- The type and the date of seismic acquisition.
- The type and the year of processing applied to the data.
- The inventory and respective quality of Pre-Stack data (gather, offset/angle cubes, intercept, gradient, etc...).
- The seismic image quality at the objective level.
- The preservation quality of the seismic amplitudes and the estimation of the phase of the input seismic data, (being ideally zero phase) through well tie for example.
- The spatial coverage (bin size, maximum offset, spacing of traces, etc...), as well as the horizontal and vertical resolution (dominant frequency, tuning thickness, etc...).
- The key petroelastic properties and their relationships with the various fluids. This includes the proximity and the quality of the input well data, which served as a basis for establishing the models, and in particular the quality of the density log and seismic velocity data at wells, the fluid properties, and the results of the various models compared to the calibration carried-out at wells.

Each evaluated parameter has its own weighting factor. The type of processing / migration and the seismic data vintage are of particular importance. For example, preserving the amplitude of the data that was migrated

with pre-stack depth migration algorithms in the late 90's will not typically preserve the seismic amplitudes as well as the processing available with the current algorithms. In the same manner, seismic acquisition and processing designed specifically for a given target will typically be better than a multi-client speculative seismic survey.

Overall it has been determined that the factors that have the most impact on the final value of the data quality index are the quality of the preservation of the seismic amplitudes, the bin size, the phase accuracy estimation, the vertical and horizontal resolution, the proximity of the well data (acting as control points) compared to the assessed structure, and the rock physics model accuracy.

The output of this process is the computation of a data quality index, ranging from 0 to 100%, depending on the previously mentioned factors, referring to the amount, the quality, the location (i.e. proximity) and the relevance of input data and associated studies. As an example, a data quality index of 50% will lead to a division by two of the DHI Index. In most of the projects evaluated to date (350 prospects in the consortium at the end of 2019), the data quality index lies often in a 70-85% range. From a statistical point of view, it has been demonstrated that, when this index is below 55%, the drilling success rate drops dramatically. It is therefore understood that this analysis needs to be performed carefully and objectively, as it may have a significant impact on the modification of the final Pg at the end of the process.

### 3.2. DHI Index computation

To establish the appropriate geologic setting for the DHI evaluation, the prospect is classified by its associated AVO class. The Amplitude Versus Offset/Angle (called AVO or

AVA) classification was initially developed by [Rutherford and Williams \(1989\)](#) for Classes 1 to 3, which was later modified by [Castagna et al. \(1998\)](#) to include a Class 4. [Ross and Kinman \(1995\)](#) added a Class 2P to produce five different AVO Classes (1, 2, 2P, 3, 4), as detailed in [Roden et al. \(2014\)](#) and in **Figure 6**.

As a reminder, AVO represents the variation in the amplitude of seismic reflection at zero offset (the intercept) and the change in amplitude at distances between the shot point and the receiver (the AVO gradient). AVO can indicate differences in lithology, as well as the presence of different fluid types in the rocks above ([Feng et al, 2006](#)).

AVO analysis is a technique by which geophysicists try to determine various elastic properties of the sediments, and especially the fluid content of a given reservoir. A successful AVO analysis requires special Pre-stack seismic data processing, as well as seismic modeling, in order to determine the properties of the rock with known fluid contents ([Avseth et al., 2011](#); [De Bruin, 2020](#)). Typically, the modeling results of various fluids and reservoir properties is compared to the real data, and specifically the DHI anomaly (see the next case study examples).

Therefore, the quantification of AVO characteristics is a crucial element in the overall seismic amplitude anomalies and the DHI risk assessment.

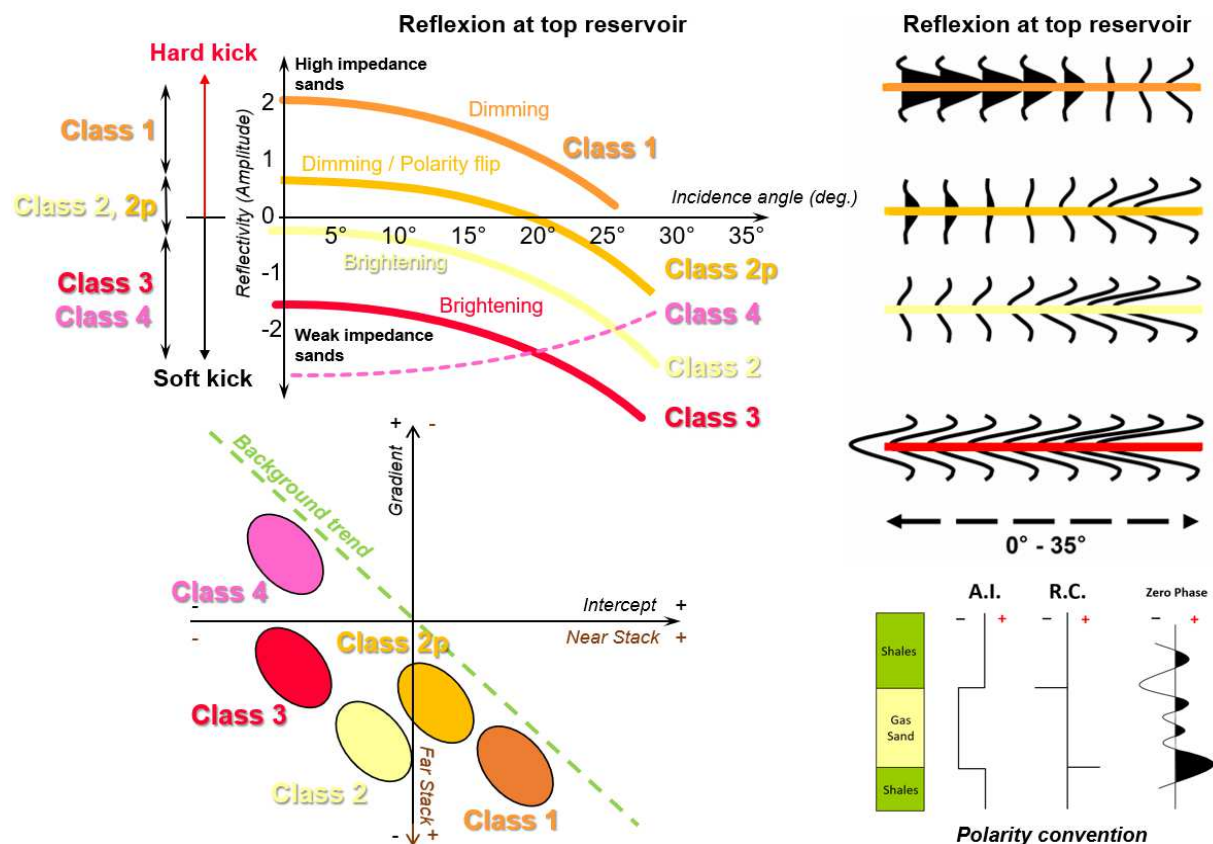


**Figure 6:** Seismic amplitude responses AVO classes as function of the incidence angle. (from [Feng and Bancroft \(2006\)](#) and [Castagna et al. \(1998\)](#), modified).

The overall DHI Index workflow consists of a series of key questions about relevant seismic amplitude characteristics, depending on the selected seismic AVO class anomaly defined for the prospect. Also considered are pitfalls, which relate to other geological and geophysical phenomenon that can produce amplitude anomalies that are not related to a commercial hydrocarbon accumulation (e.g. lithology, diagenetic effects,...).

DHI Characteristics are organized into nine categories, as detailed in **Figure 7** for a Class 3 setting. A grade ranging from 1 (worst) to 5 (best) is assigned to each DHI Characteristic. They are based upon the closest match to a

set of detailed grading standards specific to that characteristic called the Grade Descriptors.

The selected grade is then assigned a corresponding Grade Value to account for non-linearly between grades, and then multiplied by a weighing factor, which is based upon a consensus of experts judgement plus results from the Consortium’s database of calibration wells.

The sum of the weighted grade values is then normalized and re-scaled to produce the raw DHI Index, which is subsequently adjusted based upon the Data Quality Index to produce the final DHI Index.

Seismic Amplitudes categories	Seismic Amplitudes characteristics
Local change in amplitude	Amplitude difference at the evaluated structure location versus background
	Amplitude consistency within the mapped evaluated structure
	Presence of similar unexplained anomalies outside the evaluated structure
Edge effects	4 characteristics assessed (*)
Rock Physics	4 characteristics assessed (*)
Primary AVO effects	4 characteristics assessed (*)
AVO graphic analyses	3 characteristics assessed (*)
Interpretation Pitfalls	12 characteristics assessed (*)
Vertical and lateral context	4 characteristics assessed (*)
Seismic analogs	2 characteristics assessed (*)
Containment and preservation	3 characteristics assessed (*)

**Figure 7:** Seismic amplitudes characteristics for an AVO Class 3 anomaly.

Nearly 40 separate DHI Characteristics have been identified by the DHI Consortium for the seismic amplitude anomalies assessment. They are classified into nine categories. The details of the assessed characteristics (\*) cannot be given for obvious confidentiality reasons, but an example is presented for the first category.

The number of DHI Characteristics slightly differ between the five AVO classes. They are quantified one by one using a grade scoring similar to the ones done for the Initial Pg and Data Quality index assessments. Once the grade is selected, the DHI Index is calculated using the addition of all DHI characteristic grades (themselves modified by a confidential dedicated weight) ranging from 0 to 10 (respectively from No effect to Critical effect), which are in fact highlighting their relative importance.

The evaluation of seismic amplitude anomalies characteristics must always be linked to their geological environment in order to avoid errors of interpretation.

During this evaluation procedure, interpreters must answer up to 38 key qualitative inquiries (for Class 3) regarding seismic amplitude characteristics. Following the various given responses, the tool calculates the DHI Index, which represents the interpreter’s assessment that the amplitude anomaly truly is a Direct Hydrocarbon Indicator.

Theoretically, the DHI Index output can vary from -100% to +100%, but on the studied structures to date, we observe an overall general variation between -20% and +40%.

In addition, thanks to an extensive and continuously growing database within the DHI Consortium given the contribution from more than 80 E&P companies in nearly 20 years of existence, it is possible to better understand the impact of seismic amplitude characteristics and identify the ones which have the most influence on positive well results.

Indeed, the evaluations carried-out on all the calibration prospects through the years enabled a determination - from a statistical point of view (and correlated with the drilled wells success rates) - of the most significant seismic attributes characteristics, such as:

- The presence of a flat-spot in the evaluated structure.
- The conformity of the seismic anomaly to the depth map of the evaluated structure (called downdip conformance).
- The phase change of seismic character on the lower limit of the evaluated structure.
- The seismic amplitude anomaly consistency over the entire evaluated structure.
- The appropriate AVO response inside the anomaly when compared with the same reflector outside.

These very interesting outcomes over years of analyses will not be detailed in the present paper, but are described in other publications, such as [Rodén et al. \(2005, 2012, 2014\)](#) and [Forrest et al. \(2010\)](#).



Another important consideration related to the DHI assessment is the impact of the AVO DHI characteristics. Based on the DHI Consortium database, when the seismic amplitude assessment is dominated by AVO characteristics, [Roden et al. \(2014\)](#) reports a lower drilling success rate. This is typically because of uncalibrated AVO responses and the lack of stacked amplitude DHI characteristics.

In fact, seismic data yields only relative information. Rock physics gives a static view of reservoirs, irrespective of their depositional environment. Therefore, a reliable geological model is key. It needs to be established prior to the amplitude and AVO evaluations and not the other way around. In that sense, we need to avoid circular reasoning (i.e. staying away from the temptation of creating a geological model based on what we can observe when looking at seismic amplitude responses; see [Simm, 2020](#)).

It is also optimal to perform seismic amplitude evaluation based on both the reflectivity and the impedance domain, on both partial (i.e. near, mid, far) and full offset/angle domains, as well as on both top and base potential reservoir reflectors. The goal is to avoid any pitfalls in the interpretation process (i.e. inconsistencies due to tuning or other seismic artifacts; [Houck, 1999, 2002](#)) and to ensure consistency in the interpretation and the resulting geological model.

Moreover, as raised by [Simm \(2017, 2020\)](#) and [De Bruin \(2020\)](#), a clear consistency must be shown between the observed attributes and the rock physics to demonstrate a likely HC interpretation. For that purpose, the calibration and the distance to control-points is paramount, as well as the generation of alternative models to challenge our vision (pitfall analysis is there an important step). The non-presence of AVO or amplitude anomaly needs also to be explained in the geological models (e.g. a non-flat-spot presence due to limited sand thickness).

All these potential issues are raised during the DHI Index assessment procedure, in order to ensure a systematic, consistent, rigorous and auditable risk evaluation review. The goal is to not neglect any pertinent geological nor geophysical information necessary for a proper prospect evaluation.

#### 4. Final Pg computation

As detailed in the previous sections of this paper, we have to this point estimated the Initial Pg without considering the seismic amplitude support over the identified prospect of interest, and then calculated the DHI Index, which acts a quantitative estimate of the reliability of the seismic amplitude anomaly as a fluid indicator.

The final calibrated probability of geological success (called revised Pg in [Figure 3](#)) is based upon the Initial Pg and this weighted DHI Index. The calibration method to be used is still subject to several approaches within the DHI Consortium, as well as in the literature (see [Houck, 1999](#); [Simm, 2017](#); [Rühl and Samuelsson, 2017](#)) and varies among E&P companies. Some recommend applying empirical methods or crossplot techniques of Pg elements ([Forrest, 2010](#); [Forrest et al., 2010](#)). Others are proposing various Bayesian equations integrating the results of drilled prospects ([Stabell et al., 2003](#)).

In relation specifically to the DHI Index, it has been proven that it has a strong correlation to the success rate. The more the most highly-ranked DHI characteristics are observed on the evaluated prospect (the ones presented on the previous chapter and in [Figure 7](#)), the more likely the revised Pg will be increased, as they are directly associated with the total Petroleum System elements defining the assessed structure.

Based on [Roden et al. \(2012\)](#) and the 2019 DHI Consortium results in [Figure 8](#), when a prospect has a DHI Index over 12%, almost all the drilled wells give positive results (i.e. technical or commercial discoveries). On the opposite side, when the DHI Index is lower than 0%, almost all the drilled prospects are dry. The calibration and normalization (due to irregular sampling) of the available DHI Indexes, based on drilling results, is seen to efficiently overcome the interdependencies of the seismic amplitude characteristics of a given prospect, in order to generate the revised Pg.

To date, three different DHI Index calibration methods are available in the DHI Consortium tool, ranging from graphical calibration curves to more statistical Bayesian methods. The latter are supposed to be the best statistical theoretical solutions but are considered so far not optimal probably due to both the limited database and the important recent evolution of the Initial Pg assessment procedure (database update ongoing). The optimum gage of a calibration's accuracy is when a crossplot of the actual success rate versus the calibrated final Pg produces close to a 45°line.

Whichever calibration method is employed, it should be applied consistently to the overall exploration portfolio. This includes Value Of Information (VOI) decisions for acquiring additional or enhanced information, and eventually for optimal drilling decisions among the ranked portfolio.

We will now tailor this step-by-step assessment procedure methodology with a seismic amplitude-supported Nile delta case study, starting from the Initial Pg evaluation, the DHI Index calculation, until the final generation of the final revised Pg.

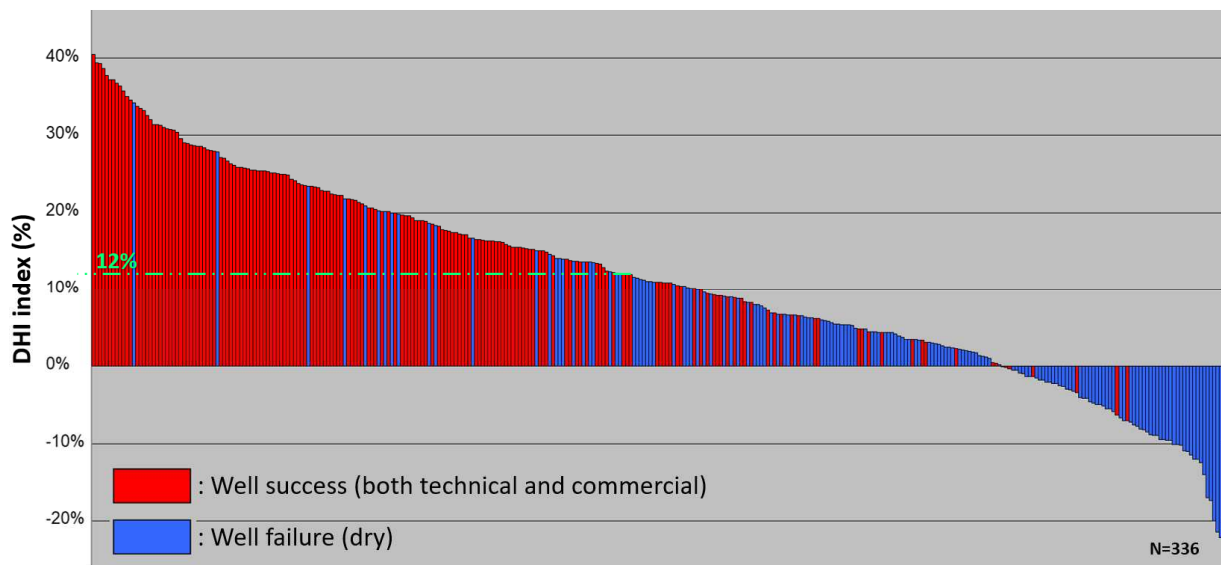


**Figure 8:** Drilling results of Prospects versus DHI Index for the DHI Consortium Database

This graph, which was extracted from the DHI Consortium database, shows each of the Consortium's 336 calibration prospects (as of 2019) as a vertical bar colored red for geological / technical successes or blue for dry holes. The prospects have been sorted left to right from largest DHI Index to smallest.

We can observe some false positives and false negatives in the well results, due to particular pitfalls, such as low saturation gas, seismic artifact responses and other seismic data quality related issues. For prospects with DHI Indexes above 12-15%, most of the wells are successful. For wells with DHI Indexes below 12% the positive impact of DHIs diminishes including negative DHI Indexes.

## 5. Case study

### 5.1 General location and regional background

The studied area is located in the western part of the offshore Nile Delta, close to the Rosetta Nile river mouth (Figure 9).

The Nile delta basin covers an extensive area including onshore, shelf and deep-water environments. It is a giant hydrocarbon-rich province ideally situated for market within the circum-Mediterranean region, and the most active gas exploration and development province of Egypt.

There, numerous types of HC plays (Figure 9) provide a multitude of opportunities in both structural and stratigraphic traps (Aal et al., 2006; Dolson et al., 2002; Dolson, 2020).

The explosive exploration growth that occurred in this region has been largely dominated by the Post-Messinian formations (Rio et al., 1990; Aal et al., 2006; Barsoum et al., 1998; Dolson et al., 2002; Dolson, 2020; Cozzi et al., 2017; Ibrahim et al., 2010; Nabawy et al., 2018).

After the first onshore discovery in the Upper Miocene Abu Madi formation in 1966 by IEOC, exploration progressively moved to the offshore domain, first focusing on Pliocene El Wastani and Kafr el Sheikh (KES) targets, with Scarab and Saffron fields discovered in 1988 (Abd El-Hafez et al., 2014; Moktar et al., 2016). The deeper pre-Messinian discoveries include Raven in 2004 and Satis in 2008 (Whaley, 2008). The most recent Cretaceous play includes the ENI Zohr discovery in 2015 (Esestine et al., 2016), which opened new horizons for further exploration activities.

The evaluation of this case study began in 2006 when the E&P company entered the first exploration phase of the exploration concession, with commitments for one well and 300 km<sup>2</sup> of 3D seismic to acquire.

The Geological and Geophysical (G&G) studies were first focused on the Plio-Pleistocene geological targets, and especially on the southern part of the concession, where water depths are below 50 to 60 m. This area was only covered previously by sparse and poor to fair quality 2D seismic surveys.



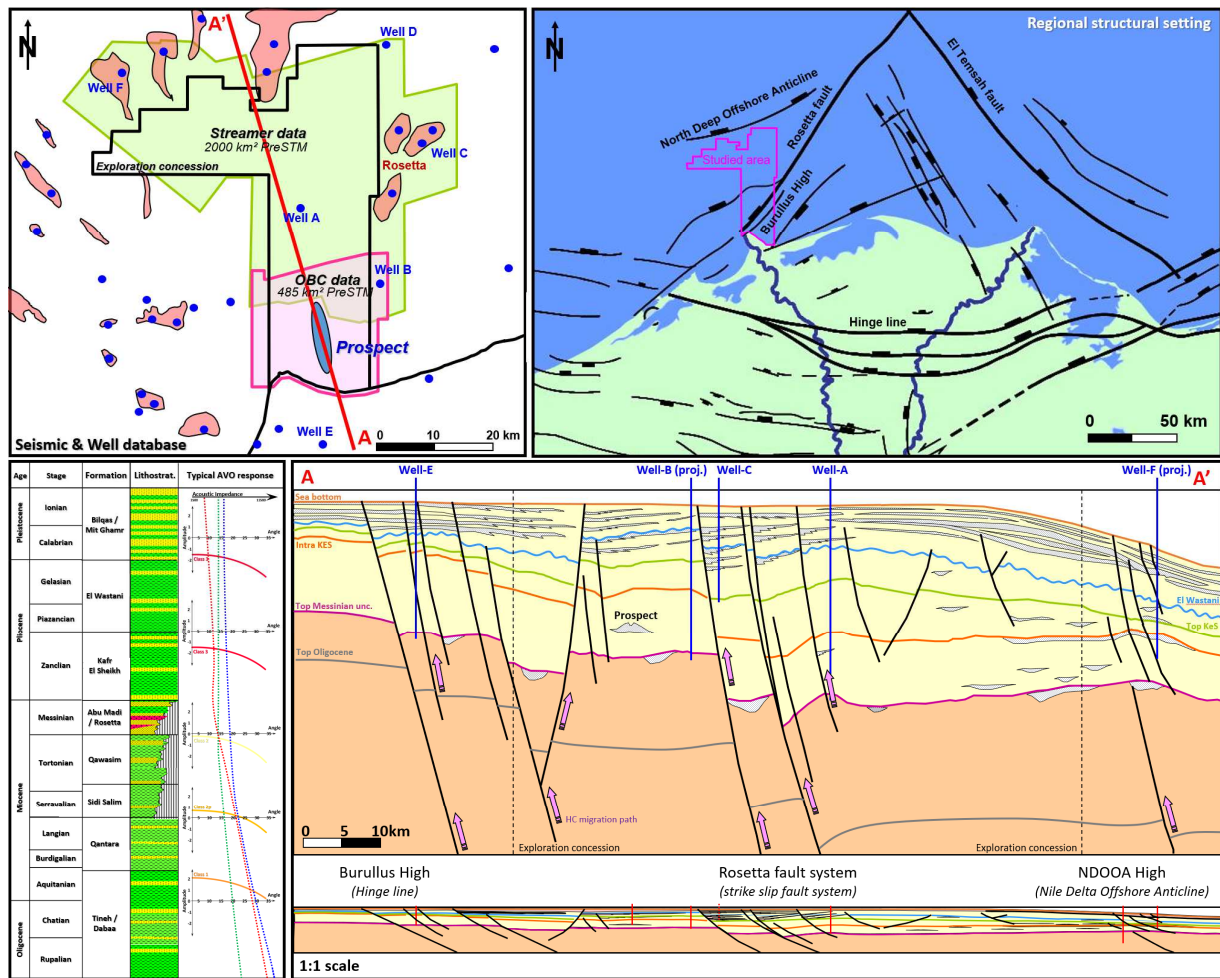


**Figure 9:** General setting of the study area.

The upper right figure shows the exploration concession location in the offshore Nile Delta and the general structural framework of the studied area. The upper left figure represents the available well and seismic database. The lower right figure highlights the main play fairways of the offshore Nile Delta and the location of the evaluated prospect. The lower left figure represents the Nile Delta stratigraphic chart from Oligocene to recent. The Acoustic Impedance and associated AVO behavior at various depths are detailed.

From a structural perspective, the studied area is dominated by the subduction of the African plate under the Eurasian plate. This was due to a back-arc extension associated with the rollback of the retreating Calabrian-Tethys subduction zone (Granado et al., 2016) that has been progressing steadily since Cretaceous times (Aal et al. 2006; Ibrahim et al., 2010). These events resulted in the creation of a complex triangular mega-structure (Figure 9) characterized by three major fault trends that form the boundaries of the Nile Delta (Biju Duval and Montadert, 1978; Kellner et al., 2009, 2018).

To the South of the delta, a large E-W trending fault system (called the Hinge line) delimits the continental shelf to the South. It is characterized by a shallow basement and the presence of faulted blocks from the subsiding Nile delta depositional system to the North, which is dominated by an important subsidence evolution and forming a thick Tertiary sedimentary pile. The eastern part of the delta is crossed by a major NW-SE strike slip

fault corridor called the Misfaq-Bardawil or the Tomsah fault trend (Ahmed et al., 2002; Bentham, 2011), showing a set of HC prolific parallel tilted fault blocks on its hanging wall. The western part of the delta, where the case study is located, forms the counterpart of the Tomsah fault system. It is crossed by a major NE-SW strike slip fault (called the Qattara-Eratosthenes or Rosetta fault system; Bentham, 2011; Granado et al., 2016) splitting the studied area into two different domains: the Burullus high to the South, and a wide half-graben to the North (Figure 9). The regional dip of this half-graben is to the SE, with a crest located on the NDOA (Nile Delta Offshore Anticline) high, with a thick sedimentary wedge located on the Rosetta hanging-wall fault.

These three trends are respectively interpreted as a paleo-passive margin for the Hinge line, a paleo-transform fault for the Rosetta fault, and a paleo-rifting system for the Tomsah fault (Barsoum et al., 1998; Dolson et al., 2002; Dolson, 2020).

These faults have been reactivated several times, making the tectonic history difficult to unravel, particularly following the opening of the Gulf of Suez and the N-S compression generated by the northward migration of the African tectonic plate (Aal et al. 2006; Harms and Wray, 1990).

From a stratigraphic point of view, the oldest sediments penetrated in the study area (by Well-A; see Figure 9) are Middle-Miocene delta front clastics, deposited above the Mesozoic carbonate deposits and Lower-Tertiary sediments. They correspond to the shale-prone Sidi Salim Formation. Following this open marine event, the prograding Qawasim lowstand clastics mark the first fluvio-deltaic influx in the delta area and correspond to a lowstand erosion period (Zaghoul et al., 2001; Rizzini et al., 1978; Said, 1981, 1990; Deibis et al., 1986). The Messinian section consists of basal anhydrite (Rosetta anhydrite and equivalents; Leila et al., 2020) overlain by the extensive Abu Madi Formation, which corresponds to the major second fluvio-deltaic influx. It is mainly composed of sandstones deposited in large SSE-NNW trending valleys (Wigger et al., 1996; Aal et al., 2006; Stirling, 2003). Then, a major sea level rise occurred at the end of the Messinian (El-Heiny, 1992; Dolson et al., 2002; Dolson, 2020), resulting in the deposition of deltaic to deep water sediments across the studied area throughout the Pliocene and Pleistocene.

The resulting variety of tectonic styles and depositional patterns in the area provide a broad suite of potential trap types, with both stratigraphic (incised valley infills, unconformity related pinch-outs, slope channel fills, fan lobes) and structural traps (footwall normal fault traps, hanging wall drags, rollover anticlines). For more details on the different play types, the reader may refer to the work done by Samuel et al., 2003, Boucher et al., 2004, Kellner et al., 2018 and Dolson, 2020.

## 5.2 Geological probability of success (Pg) risk assessment

### 5.2.1 The Kafr el Sheikh play

The targeted prospect is of Pliocene age and belongs to the well-known prolific Kafr El Sheikh (KES) Formation (Ibrahim et al., 2010; Rashid et al., 2018; Dolson, 2020). At the time of the prospect assessment, this play was already widely proven by numerous discoveries, especially in the north of the exploration license area, with the WDDM Libra, Scarab and Saffron fields to name a few. Nevertheless, a very limited number of discoveries had been made on the shallow Nile Delta waters by that time

The reservoir constituting this particular play is characterized by a set of turbidite channels, levees and lobes that are clearly identified on 3D seismic by amplitude anomalies and AVO effects (Samuel et al., 2003; Sharaf et al., 2014). The sands are dispersed in the mud-rich KES Formation, acting generally as effective top, bottom and lateral seals.

The turbiditic channels are known to have been initiated by the introduction of coarse sediments to the shelf edge possibly at times of relative sea level fall (Barsoum et al., 1998).

An additional important point to highlight is that a significant fraction of the reservoir is generally made of finely laminated sandstones within the levee facies, with sand streak thicknesses being below the vertical resolution of most of the logging tools (Anwar et al., 2002).

From another point of view, these reservoirs are generally located at relatively shallow depths (< 3000 m) and reveal an increasing overpressure trend with depth, up to 1.65 equivalent mud density. They tend to be under-compacted and show high average porosities (usually 20 to 26%) and high permeabilities (from hundreds to thousands of millidarcies). The temperature gradient, as often in deltaic environments, is relatively low, at 23 to 24°C/km (Elewa, 2002; Shaaban et al., 2006).

The gas is usually dry, with an average Condensate Gas Ratio (CGR) increasing with depth from 2-3 bbls/mmscf in the El Wastani Formation to more than 20 bbls/mmscf in the Sidi Salim Formation and deeper. This observation may be explained by the progressive release of the heaviest gas components along the migration path and/or the higher fraction of microbial gas present in the shallowest formations (Shaaban et al., 2006; Aal et al. 2006; Monir and Shenkar, 2016).

The thermogenic fraction of the gas is migrating through deep-rooted faults (especially NDOA and Rosetta faults; Sarhan et al., 1996; Cowan and Shallow, 1998), from deep pre-Messinian mature source rocks, likely to be Oligocene or even deeper (Cretaceous and Jurassic source rocks are well-known in the onshore Western Desert). These faults act as major vertical migration pathways, as proven in the surrounding fields where the presence of numerous small bright-spots are trapped alongside the fault cut, and the presence of gas chimneys and pockmarks (sometimes associated with mud volcanoes) that are clearly identified on the seismic data (Barsoum et al., 2002; Prinzhofer and Deville, 2013). However, these faults can locally be sealing, as proved by Gas-Water-Contact (GWC) positions in the Rosetta fields (Cowan and Shallow, 1998) and by the 3-way dips of North Idku gas discoveries.

As reservoir pressures are often close to fracture pressure, it is thought that the gas is migrating by a succession of pressure pulses. Each time the gas pressure reaches the breach-point of the weakest part of the migration route, the system temporarily opens to release the overpressure. This may explain why these major faults (like the Rosetta fault) could act together as a gas drain and be locally sealing.

In addition, a fraction of the gas has a primary microbial (i.e. biogenic) origin coming from bacterial degradation of

organic material present in the adjacent KES shales ([Monir and Shenkar, 2016](#); [Dolson, 2020](#)).

### 5.2.2 Geological prospect's characteristics

The prospect is defined as a combination of structural closure in the channel axis direction and stratigraphic closure in the transverse direction, with a lateral facies' variation from turbidite sands to marine shale. The reservoir extension (around 12 km long and 4 km wide) can be easily identified based on its lens geometry (**Figure 10**).

The structure is interpreted as a constructive channel-levees complex, with a point-source feeder system located to the SSE. The positive relief is accentuated by the differential compaction of the different facies (**Figure 10**), the channel axis being sandier than the levees.

Without taking into consideration the seismic amplitude response and associated DHI's - as described in the first part of the paper - the seismic character of the channel infill is rather complex with multiple incised surfaces, aggradational fill, and even evidence of lateral accretion on some sections (depositional/erosional channel).

The different stages of channel development can be considered in terms of slope equilibrium, with a reduction of slope gradient promoted by increases in flow size and density, and by a decrease in grain size (Samuel et al., 2003; Kellner et al., 2018).

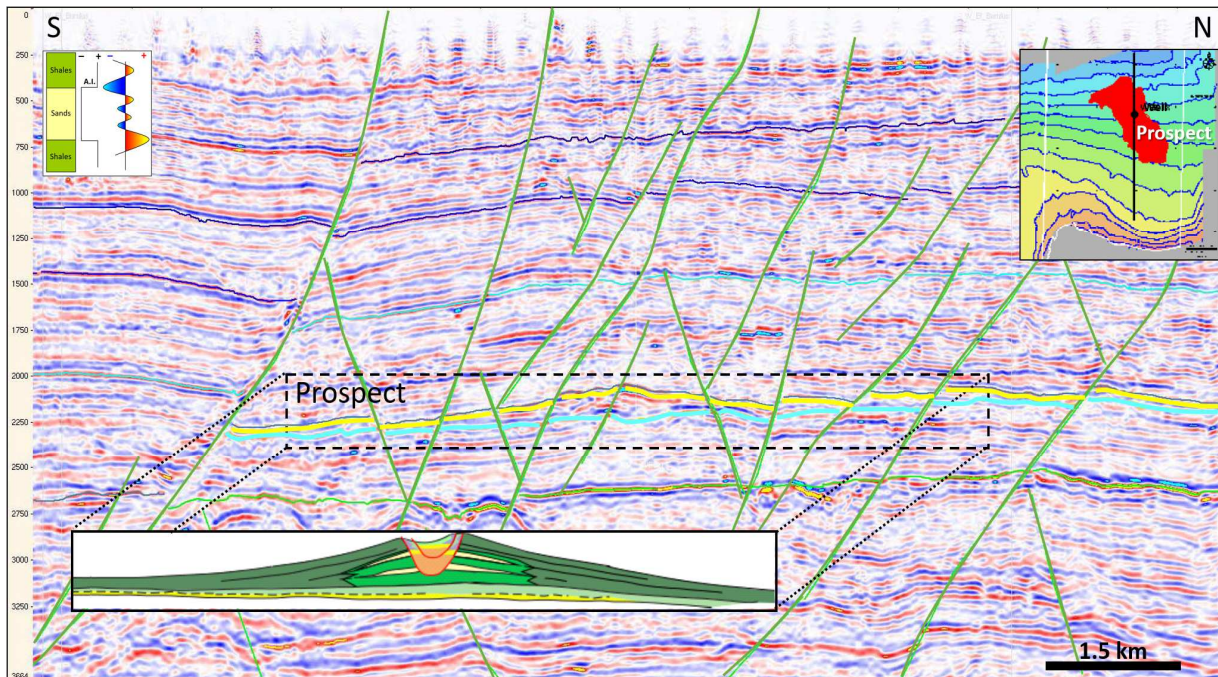


**Figure 10:** Transverse N-S seismic line through the assessed prospect.

On the Kirchhoff PreSTM full-stack seismic section extracted from the OBC dataset, we can observe a clear differential compaction geometry between the Top reservoir (soft yellow surface) and the Base reservoir (hard cyan surface). This has been interpreted as a compartmentalized complex channel levee system deposited in a NW-SE trending structural low (see **Figure 11c**), which has been later analyzed through seismic signatures in terms of depositional facies (see **Figure 14**). Its antiformal shape in time and depth (see **Figure 11a**) confirms a longitudinal structural closure. The location map in the upper right shows bathymetric contours, ranging from 0m to the South (i.e. shoreline) to 25m to the North. The white lines represent the exploration concession boundaries. The red-filled polygon shows the maximum extension of the prospect (see the Gross Rock Volume (GRV) discussion).

The base reservoir depth and thickness maps (**Figure 11b** and **11c**) show that the prospect is deposited in a SE-NW trending structural low. The top reservoir depth map (**Figure 11a**) highlights a SE-NW structural closure and the compartmentalization of the channel-levees system due to many transverse faults dissecting the prospect into several fault-blocks. The northern edge of the expected channel complex is going up to the Rosetta fault, which has proven to be sometimes a critical leakage risk for prospects in the region (Hanafy et al., 2014). The target location is lying at a depth of approximately 2000m with a

20 m water depth. The expected reservoir pressure, temperature and gross thickness are respectively 280 bar, 65°C and 200 m.

The expected average reservoir parameters are 40% for the Net to Gross ratio, and 24% for the porosity.

At the time of the analysis, one of the closest prospect analogues was located about 70 km to the NW. It is a channel complex easily identifiable on seismic (**Figure 12**) and characterized by three stacked high-porosity gas-bearing reservoirs (Pheps et al., 2003; Maguire et al.,

2009; Tawadros, 2011) which confirm the seal effectiveness for this type of combined trap. This analogue, as well as the North Idku field, have been used

to estimate the main petrophysical parameters for the volume estimations of the prospect.

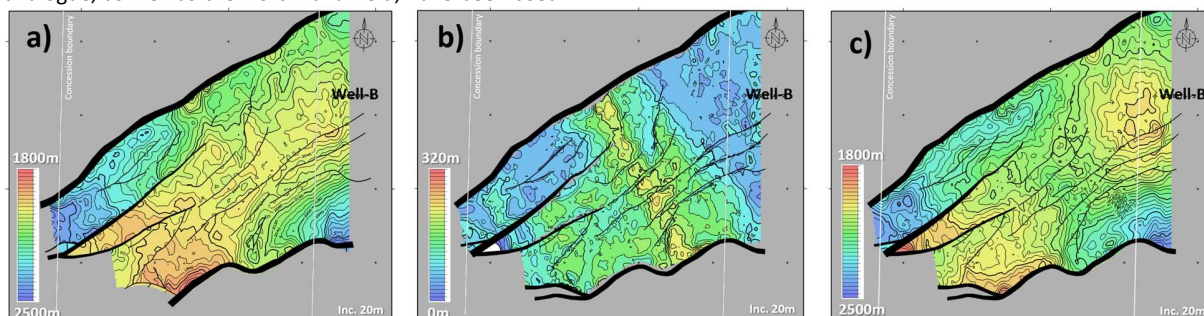


**Figure 11: a) Top Reservoir b) Reservoir thickness and c) Base Reservoir depth maps.**

The Rosetta fault represents the northern boundary (black polygon) of the prospect, while the Burullus fault represents its southern boundary. We also observe that the prospect is dissected by numerous additional SW-NE oriented minor faults.

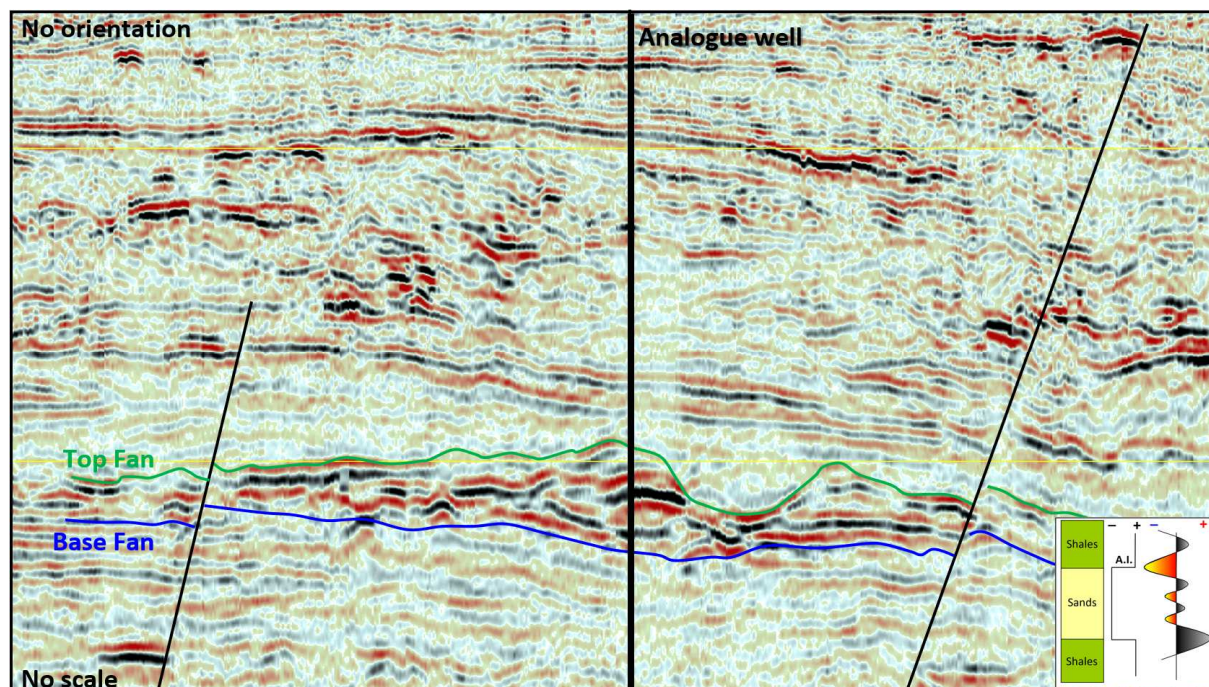


**Figure 12: Kafr el Sheikh analogue discovery used for the definition of the prospect's reservoir properties.**

This analogue (discovery) well (right panel) proved a nearly 100 m continuous gas column on a seismic amplitude supported interpreted fan/channel complex. The well also confirmed the DHI results, which predicted the possible presence of hydrocarbon in this combined structural and stratigraphic closure. Although this field lies in a more distal position than the studied prospect, both structures display important similarities (such as differential compaction and seismic internal architecture) that make the discovery a good analogue. See also Stirling (2003) for additional analogues.

The Initial Pg assessment has been calculated following the procedure described at the beginning of the publication. The key defined risk over the prospect is expected to be the top seal effectiveness, due to the presence of numerous faults dissecting the reservoir into several compartments (Figures 10 & 11). In addition, these faults are going up to the surface, and numerous small bright spots are observed alongside the main fault-cuts just above the prospect. Both lateral seals have also been considered independently in the risk assessment procedure.

An additional observed risk is the reservoir effectiveness, as no wells had yet penetrated the Kafr el Sheikh sands in such a proximal paleogeographic location. Indeed, all the analogue wells drilled within this play are located more than 20-25 km northwards, and the closest well (Well-B) did not show any effective sands in the KES Formation. As a result, without taking into consideration the seismic amplitude support, we obtain an Initial Pg of 19%, which is already believed to be a rather good score for this type of combined-trap prospect.

In terms of independent supporting evidence, if the seismic amplitude was not present, we would still recognize the interpreted feature as having reservoir present, but we would not recognize this feature as a valid combined-trap, and therefore would not consider this location for drilling. Thus, amplitude support is of particular importance for this prospect. That is what we will now detail in the last part of this publication.

### 5.3 Seismic amplitudes risk assessment

Following the evolution of seismic data acquisition and processing techniques through the years, the hydrocarbon exploration in the offshore Nile Delta - and more largely in the great Eastern Mediterranean Sea - has increasingly been focused on Mio-Plio-Pleistocene gas-bearing sands, highlighted by fair to good seismic amplitude and DHI supported prospects (Galbiati et al., 2009; Haffinger et al., 2015; Pettinghill et al., 2019).

Nevertheless, as highlighted by Hanafy et al. (2014, 2018) and Firinu and Sahadic (2014), evidence of amplitude anomalies interpreted as DHI's in this region did not always lead to positive results. Therefore, a proper seismic amplitude assessment for reliable and consistent prospect evaluation within these plays are of primary importance.

We will now detail the two-steps process, discussed previously in this publication, in order to calculate the DHI Index, weighted by the available Data Quality index.

#### 5.3.1 Data Quality index assessment

As discussed, the amount and quality of direct data, as well as their proximity to the mapped prospect are critical for the evaluation. In order to properly risk seismic amplitude anomalies, it is necessary to evaluate the quality of the seismic data and the nearby relevant rock physics well information. Indeed, the quality and proximity of known density and P and S-wave velocity information are key because they relate to the interpreter's confidence level of the associated acoustic response of the prospective anomaly.

As such, good well control not only helps in better defining the geological model, but also provides more accurate input into AVO, fluid replacement, resolution and tuning modeling. The latter two are of particular importance for DHI supported Nile Delta reservoirs (Galbiati et al., 2009; Fervari and Luoni, 2006; Nashaat et al., 2001).

In 2006, 485 km<sup>2</sup> of 3D seismic were acquired over the southern area of the license, which was not covered by existing 3D seismic survey. It was the first 3D OBC survey shot in the Western offshore Nile Delta. It also fulfilled the seismic commitment of the first exploration phase. In addition, the entire old vintage northern 3D seismic and a part of the 2D seismic available within the exploration concession were reprocessed. The final reprocessed seismic cubes and new seismic were delivered in May 2007.

At prospect location, only the 3D OBC seismic data and very limited quality 2D seismic surveys are available. The acquired OBC survey is in fact a sparse OBC with the following main characteristics: 50 m trace spacing, 600 m line spacing, source line length of 4800 m, a shot point

(SP) every 25 m (i.e. 192 SP per line), which gives a 52-fold in 25 x 12.5 m bins.

The benefits of such a sparse acquisition are discussed in Olofsson et al. (2012), Lecerf et al. (2017) and Long (2019). The acquisition perimeter has been extended to the Eastern neighboring block in order to have a well-tie (Well-B) within the 3D OBC survey (Figure 9).

Processing has been performed using Kirchhoff Pre-Stack Time Migration (PreSTM), using both hydrophones and geophones information. Available offset stacks (near, mid and far) and raw angle gathers (up to 31°) enabled a reliable and robust quantitative AVO interpretation for the Plio-Pleistocene targets, although we are unsure that the data is totally zero-phased, as the well-tie result done on Well-B was not totally conclusive.

The average dominant frequency within the zone of interest varies from 15 to 20 Hz. Tuning thickness has been estimated, from wedge modeling on both full and far offsets data (Figure 20), to be at around 10 to 12m gross reservoir thickness.

These results - and thanks to both long offsets and wide azimuth content - show that the final processed data are satisfactory, despite strong noise on raw data. The imaging result is good down to about 6 s TWT, enabling a detailed seismic interpretation from Pleistocene to Oligo-Miocene.

An additional higher frequency streamer seismic survey, reprocessed in 2007 and covering the northern part of the exploration license (Figure 9), has been used for detailed AVO analyses tied to key wells. The study results (as the background trend) have been later applied to the OBC seismic data, leading to rather important conclusions at prospect location. This will be detailed in the next chapter.

Regarding the well database, only one well (Well-A; Figure 9) was drilled (in 1985) in the concession. It was dry. But we have also access to a dozen other wells in the area: Well-B is covered by the OBC data. The Rosetta field wells, Well-D and some WDDM wells are also available. They are covered by the 3D streamer seismic dataset (Figure 9). Log data have variable quality, but sufficient enough to perform reliable fluid substitutions and other relevant geophysical studies.

According to the available input data and performed geophysical studies, we calculated a Data Quality index of 74%, which reflects a relatively good data adequacy between the seismic and the rock properties information. This value will later be applied to the DHI Index, before generating the revised Pg.

### 5.3.2 Seismic amplitudes assessment: the DHI Index

Most Plio-Pleistocene discoveries located in the Nile Delta are DHI supported (Deibis et al., 1986; Hashem et al., 2010). In the early exploration times of the Nile Delta, DHI interpretation was only limited to conventional bright spot observations (Hanafy et al., 2014).

In this paper we are using various DHI analyses techniques, combined with rock physics and additional geological studies in order to finetune and derisk prospects within this particular play (see details in Helmy and Fouad, 1994; Sarhan et al., 1996; Harwood et al., 1998; Cowan et al., 1998; El Maghraby et al., 2010).

Once all the key DHI characteristics are defined on the prospect, the remaining challenge is to efficiently estimate the uplift or downgrade factors that will need to be applied to the Initial Pg, in order to obtain a final Pg value that will

be then used for economic valuation and ensuing relevant strategic decisions.

Using the Seismic Amplitude Analysis Module (SAAM) developed in the DHI Consortium, we initially input a description of the prospect including play type, basin, location information and specifically its main strengths and weaknesses, that can be used as a basis of additional finetuning studies. This information is helpful for further derisking of the prospect, before making any drilling decisions.

The expected top reservoir is defined on the full-offset stack as a high-amplitude soft event, associated with a decrease of acoustic impedance (Figure 10). The outline of the channel complex is also easily identifiable on the various seismic amplitude maps (Figure 13).

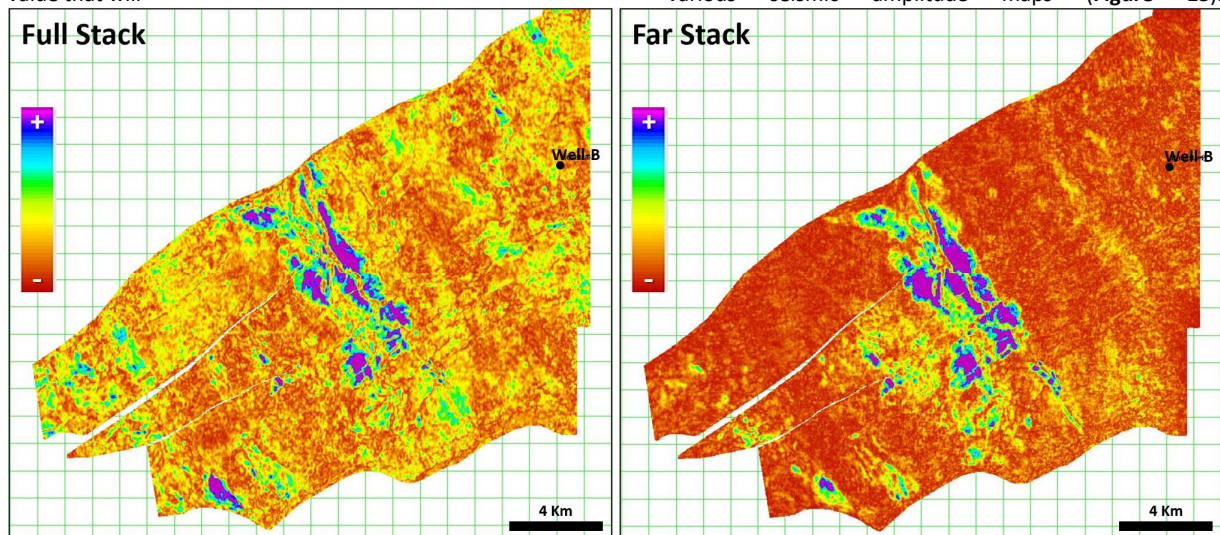


**Figure 13:** RMS amplitude maps extracted on the whole reservoir section from Full Stack and Far Offset cubes.

The Kafr el Sheikh (KES) formation gas-bearing sandstones are generally well imaged within the Nile delta using seismic amplitude extractions, as their acoustic impedance signature is considerably lower than the surrounding shales (Cross et al., 2009b). They also generally offer a fine-scale sand body architecture that can help the interpretation process and confirm the geological model.

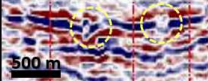
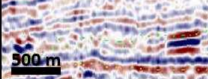
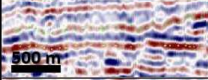
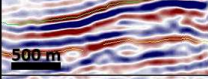
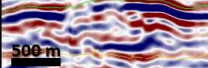
An attempt at seismic facies identification was done, based on the internal texture configuration and the external shape of seismic reflections (Figure 14), similar to the work produced in other petroleum provinces by Cross et al. (2009a, 2009b) and Gong et al. (2013). The limitation of this analysis lies on the fact that no well calibration showing similar sand body features is available within the OBC seismic survey.

Nevertheless, this analysis and associated results are similar to what we can observe on analog fields, as in the Abu-Sir, Libra, Taurus and Sequoia fields, for both Plio-Pleistocene KES and El Wastani reservoirs.

Within the prospect, we have been able to identify up to five different types of seismic facies that have been interpreted in terms of depositional environment, as shown on Figure 14.

Using various seismic amplitude maps (Figure 16), it has then been possible to produce a depositional history for this channelized turbiditic complex (Figure 15 and 16). These conclusions have been further validated using spectral decomposition tools (not detailed in the present paper).



	Seismic configuration	Seismic texture		External shape	Termination	Seismic facies example	Depositional model interpretation
		Amplitude	Continuity				
e)	Chaotic	Low-None	Transparent	Irregular	Erosion		Plugged channels
d)	Subparallel	Variable	Discontinuous	Lens	Downlap		Small aggradational non-amalgamated channels
c)	Parallel to subparallel	Low	Semi to Continuous	Sheet	Onlap		Laminated levees (less proximal, thin bedded)
b)	Parallel to subparallel	Mod-High	Continuous (flat)	Lens	Onlap		Proximal levees (thick bedded) / Basal lobe
a)	Subparallel	Mod-High	Semi Continuous (shingled)	Lens	Erosion		Channel complex with laterally amalgamated channels

**Figure 14:** Major seismic and depositional facies identified at prospect location.

From base to top, we encounter: **a)** a moderate seismic amplitude with semi-continuous to continuous low-dipping to flat reflectors, interpreted as a basal lobe ; **b)** a high to moderate seismic amplitude, with discontinuous and shingled reflectors, mainly located in the expected channel axis, and interpreted as amalgamated channels (i.e. channels complex) ; **c)** high to moderate amplitude continuous reflectors located on both sides of the channel axis, interpreted as proximal levees formed from the overspill of channelized turbidity currents ; **d)** distal levees (low seismic amplitude continuous reflectors) located in the extension-end of the proximal levees ; **e)** a transparent seismic facies (outlined in yellow) located on the channel axis, interpreted as the last shaly-channel, which plugs the system.

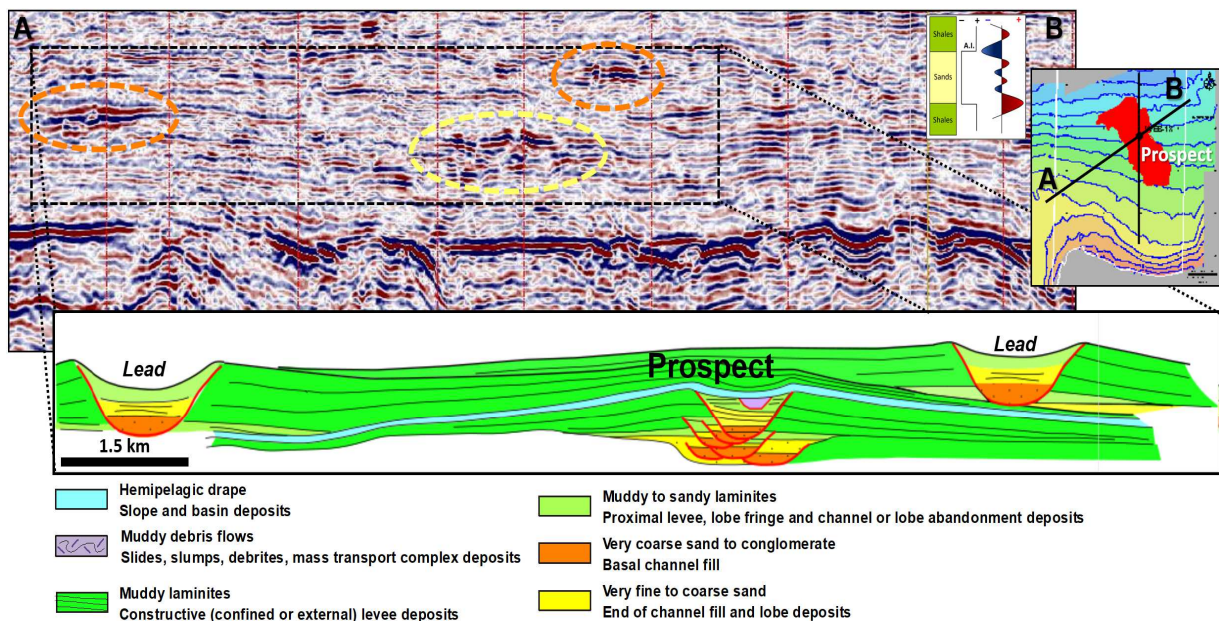


**Figure 15:** General depositional setting of the assessed prospect.

This seismic line extracted from the Kirchhoff PreSTM OBC full-stack seismic survey shows the general depositional model scheme extracted from the interpretation of the seismic facies at the prospect location. When complete, the interpretation has been extended to additional leads in order to understand the geological model in its globality. There, we can observe the assessed prospect in the center of the random line (outlined in yellow on the seismic section) and two additional amalgamated channel complexes, located on each side of the prospect (outlined in orange on the seismic section), and expected to be deposited by lateral accretion, starting with the studied prospect, then with the western lead, and eventually with the eastern lead. These leads are also nicely visible on the RMS seismic amplitude maps in **Figure 16b** and **16c**.

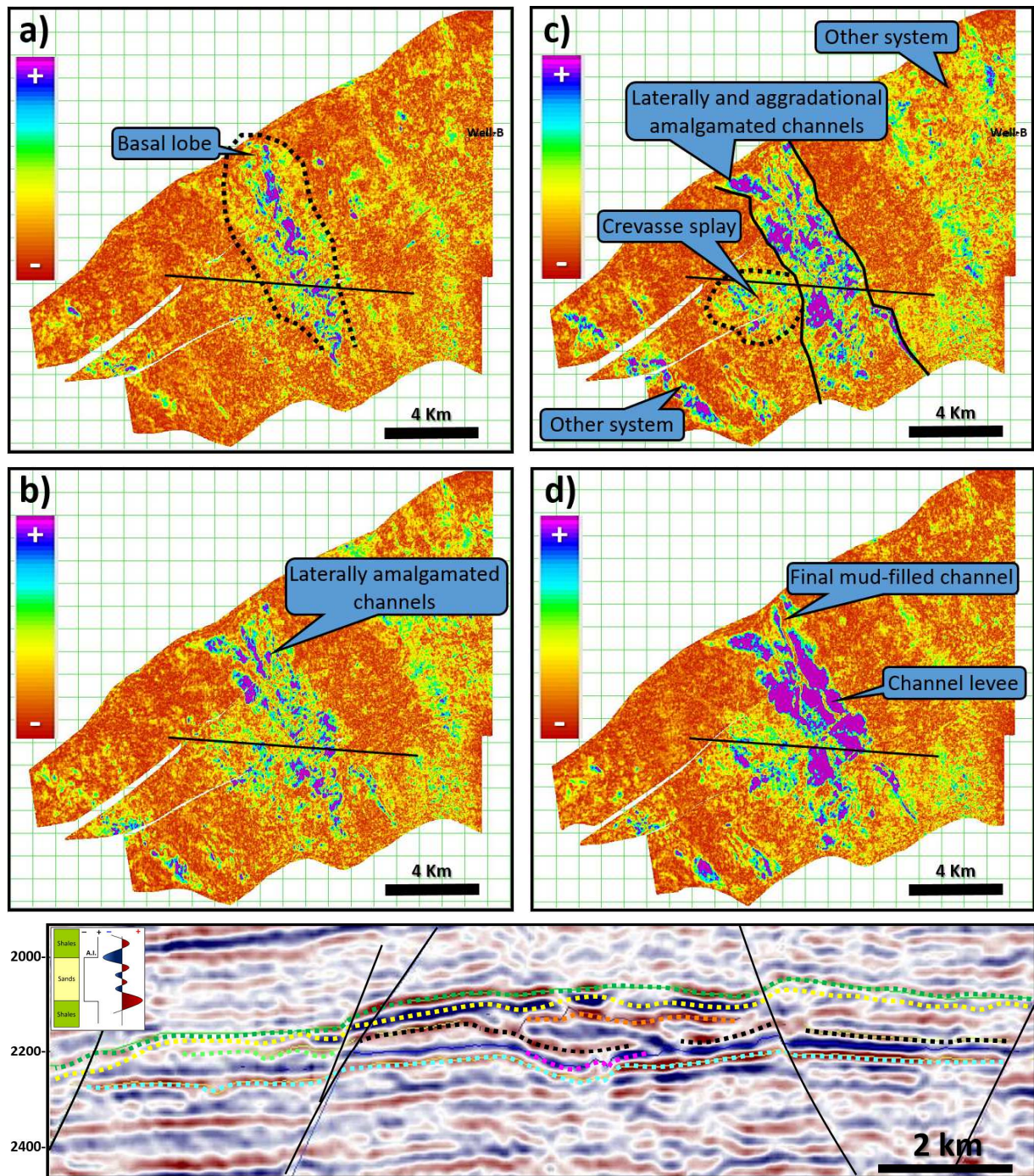


**Figure 16:** Sequential seismic amplitude maps and interpreted depositional steps of the channelized complex.

These RMS seismic amplitude maps have been extracted from the Bottom (in cyan) to the Top (in yellow) of the expected reservoir. They are interpreted in a four-step depositional process: **a)** Step 1: Depositional lobe and first downcutting erosive channel in a mud-dominated low-dip submarine slope. On the RMS amplitude map, it is expressed as a relatively uniform moderate amplitude zone with a tongue shape. The seismic E-W striking section shows an overall tabular geometry (in pink). A sinuous channel incises this depositional lobe and is interpreted as the first erosive channel of the system, in which only the erosive part is preserved. **b)** Amalgamated channels developed during step 2. The seismic amplitude map shows several high amplitude and elongated objects, which are interpreted as an amalgamated sheet-like arrangement of numerous channel bodies. On the seismic section, they correspond to discontinuous high amplitude reflectors (in black). **c)** During step 3, a moderate to high amplitude lobate shape appears beside the channel belt. On the seismic section, it is characterized as a moderate to high-amplitude continuous reflector (in orange and green). It may be interpreted as a crevasse splay (also called lateral splay in the literature; [Cross et al., 2009a](#)). **d)** Step 4 corresponds to the last evolution of prospect deposition, defined as the last elementary channel, which is plugged with shaly material. It may correspond to a stop of the source of sediment dynamics, or the cessation of the migration of the system. It is important to recall that these maps can only be used as approximations, as no direct well-tie is available. The line location is presented on the figures.

AVO is known as a robust tool for fluid discrimination in the Nile Delta area, and more particularly for the Kafr el Sheikh (KES) Formation (Hashem et al., 2010; Hanafy et al., 2014).

The KES sands are indeed known to behave as an AVO class III when charged with hydrocarbons (HC). There, the HC sands are softer than the surrounding shales, and they increase in negative amplitude as offset increases (see Figure 6 and 19). In addition, these AVO anomalies are often characterized by the presence of bright-spots on stacked seismic data.

For the AVO analysis performed on the prospect, we used the Kirchhoff PreSTM offset stacks, the angle gathers, as

well as the gradient and the intercept cubes provided by the processing contractor. As indicated in Figure 17 this prospect is characterized by a low to moderate negative intercept and a moderate to large negative gradient.

We also notice a clear brightening at the top of the reservoir from Near to Far offset data, in both the gathers and angle stacks (Figure 18 and 17). A velocity decrease at the prospect location is present on the seismic velocity cube, but no sign of pull-down or clear frequency decrease has been identified. The latter can be explained by the fact that we do not expect very thick sands at the prospect location.

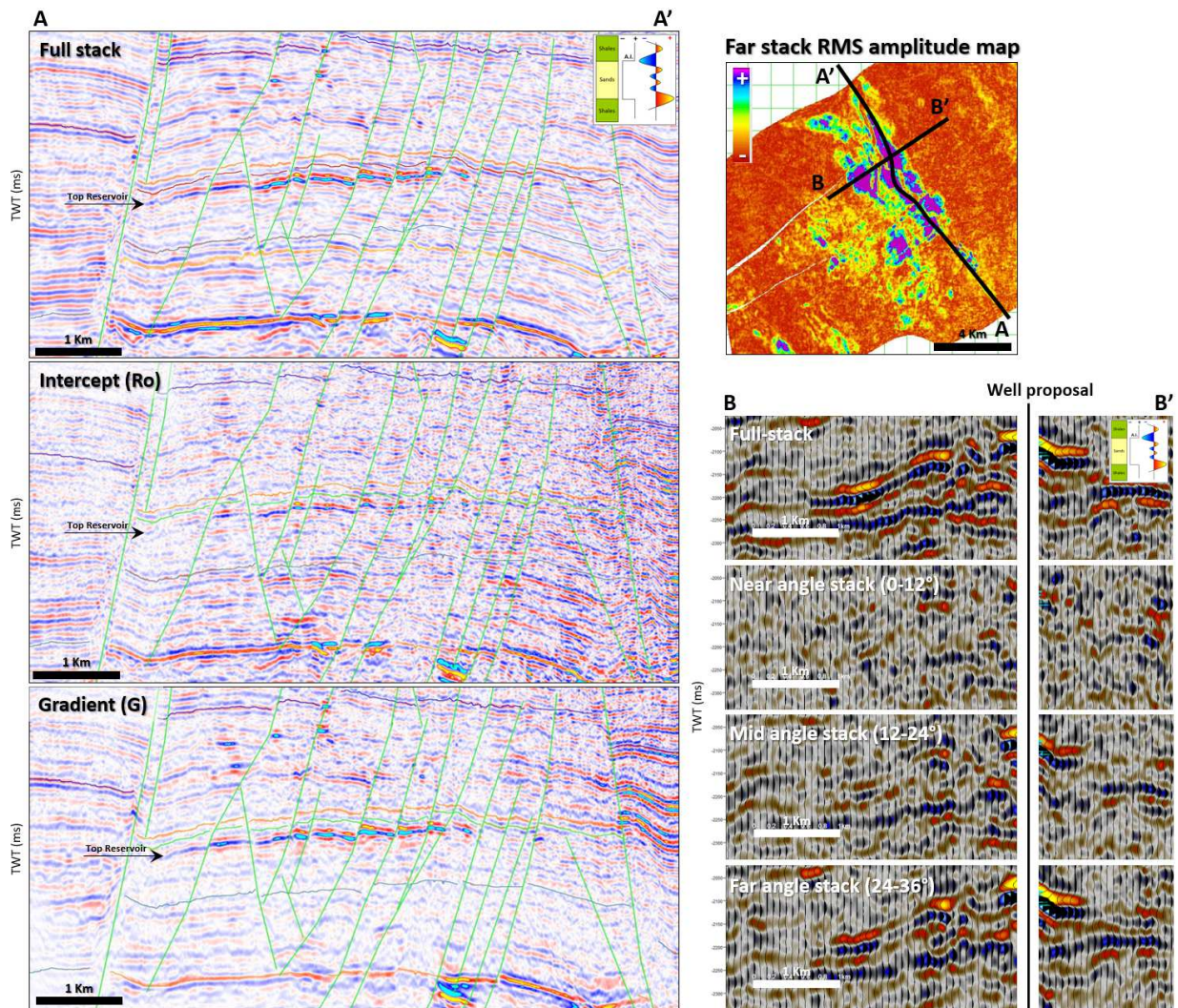


**Figure 17:** Reference AVO seismic section products through the studied prospect.

The left figures are respectively from top to bottom the Full-Stack, Intercept and Gradient reference seismic random lines of the assessed prospect. They are oriented longitudinally through the prospect channel axis. We can observe a clear Top reservoir response, which is suddenly disappearing (i.e. seismic amplitude shut-off) below a certain TWT depth. This observation will be discussed later in the publication. The right figures present a NE-SW seismic random line, showing a clear brightening from Near (where no seismic amplitude anomaly can be observed, i.e. similar to the surrounding KES shales) to Far (where the observed seismic amplitudes are five to six times brighter compared to the surrounding shales).

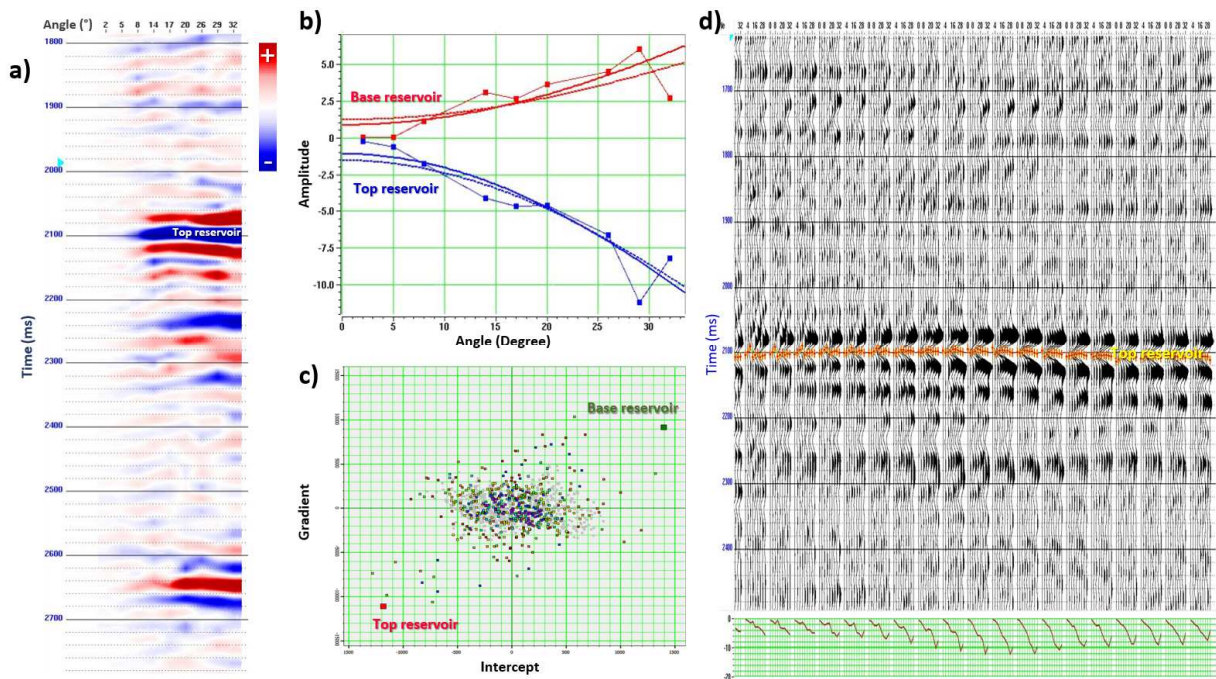


**Figure 18:** Gathers analysis over the studied prospect.

The left figure **a)** is a super-gather extracted in a centre of a levee deposit. Maximum angle is 32°. Figure **b)** represents the Angle versus Amplitude crossplot. There, we can observe that the prospect is characterised by a high negative gradient, highlighting a clear Class III AVA effect. This is validated by the Gradient-Intercept crossplot **c)** extracted from the super-gather. The shale trend (see detailed explanation later in the paper) is not very well defined, but Top and Base reservoirs are displayed clearly away from it, confirming the observed AVO effect. The right figure **d)** highlights gathers AVO effect variation throughout the prospect, with some noticeable seismic amplitude variations, even if always characterised by a Class III AVO.

In order to validate these observations, we performed a fluid substitution study. **Figure 19** highlights the AVO theoretical response of the KES sands for the different fluids. Additional sensitivity studies have been done using different porosities and reservoir thicknesses. All results reflect what has been observed on real seismic data. We can therefore conclude that the prospect is in an AVO class III setting.

In the risking process, interpreters should be aware of certain limitations. One is that, as discussed earlier, AVO analysis cannot discriminate between low and high gas saturation.

Secondly, the available OBC product has clear fluid prediction limitations. This is mainly due to its low frequency content (15 Hz to 20 Hz in average at prospect location) and low signal-to-noise ratio, which can lead to non-robust estimates of intercept and gradient. The seismic resolution is therefore important to check, in order to avoid any issue in the evaluation of potential thief sands at prospect location, as highlighted by [Anwar et al. \(2002\)](#) and [Houck \(2002\)](#). The performed wedge modeling (**Figure 20**) indicates a detectability threshold (i.e. tuning thickness) of 10 to 12m gross sands (i.e. 4 to 5 m net sands) with a stable signature, using both full and far stack traces.

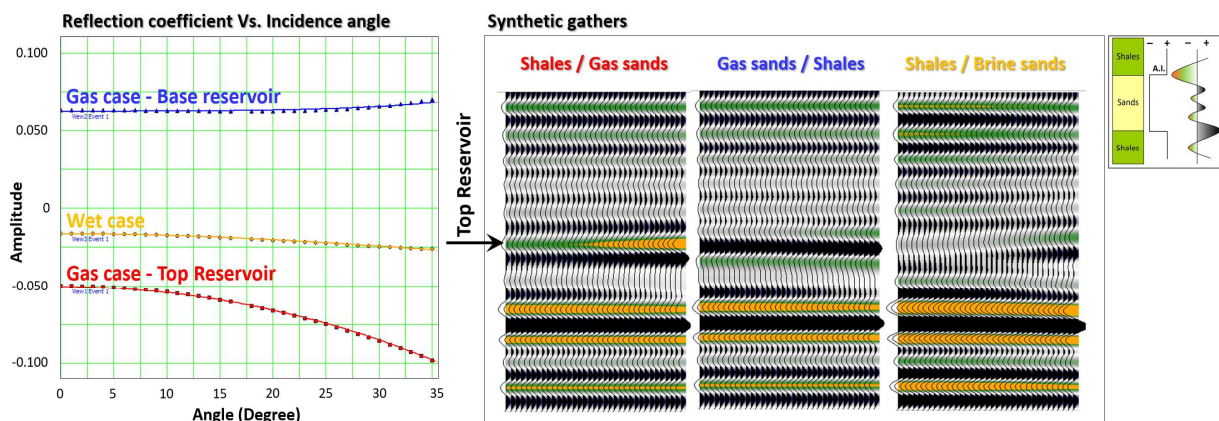


**Figure 19: Reservoir AVO theoretical response at prospect location.**

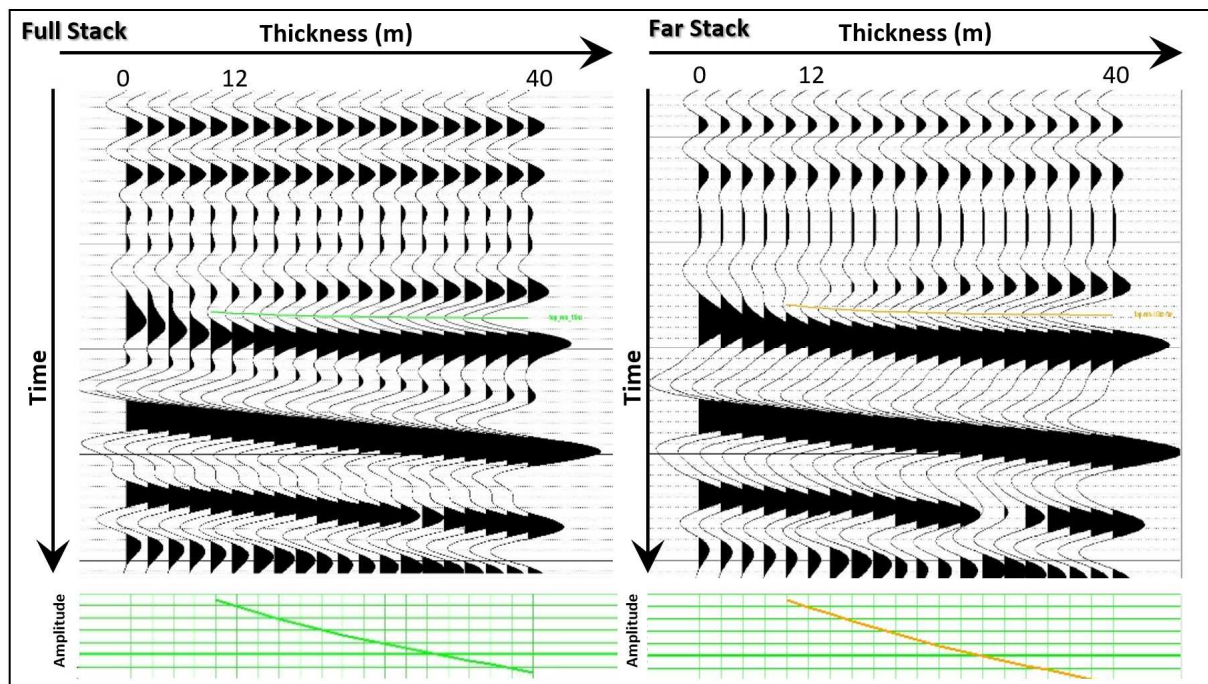


**Figure 20:** Seismic wedge modelling over the prospect on Full (left) and Far (right) stack traces.

Hanafy et al. (2014, 2018) report that the key seismic amplitude and DHI elements that are related to successful drilling cases within the Nile Delta are the following:

- The presence of bright spots in full-stack, associated with important brightening from near to far stacks, as observed in all the discovered KES fields (Sharaf et al., 2014).
- A seismic amplitude conformance to structure, as observed in the Ha'py field (Wigger et al., 1996).
- For thick reservoirs, the presence of flat-spots, polarity reversal, frequency and amplitude reduction within and below the reservoir, as well as velocity sag or pull-down, as observed in the Rosetta field and the Fahd structure (Cowan and Shallow, 1998).
- The presence of a gas chimney in the close structure vicinity, as observed in Saffron and Habbar areas (Barsoum et al., 2002).
- A sharp seismic amplitude termination against faults (when present), as observed on the Seman and Darfeel structures (Hamimi et al., 2020).

These observations are in-line with what is observed in other clastic domains (Nixon et al., 2018 and Wojcik et al., 2016).

At the prospect location, the most relevant DHI characteristics that define the prospect are the presence of a strong bright-spot at the top of the reservoir, a sharp seismic amplitude shut-down at the edges of the structure, as well as a clear AVO response compared to the background (see Figure 24 for a detailed summary). Nevertheless, we do not observe a clear flat-spot

response (that particular issue is discussed later), polarity reversal, velocity sag or frequency loss.

From the gradient and the intercept attributes, we generated a fluid cube to help discriminate the zones where gas sands are more likely to be present (Davies et al., 2003; Connolly et al., 2005). From a mathematical point of view, the fluid cube is a linear weighted combination of both gradient and intercept cubes (i.e. with this method, we reduce the two observables into one attribute).

In order to generate a fluid cube, we must follow a three-step process:

- The first step is to define the wet trend (background trend) by selecting an area where we are sure that it contains only dry rocks (i.e. water-filled reservoirs or shaly interval).
- The fluid cube is then generated by selecting the seismic information that will have the most negative values (i.e. the farthest off the wet trend; refer to Figure 6). Indeed, negative values usually reinforce the probability of presence of hydrocarbons in the analyzed sands.
- The last step is a validation process using all available well data, in order to check that the response is compliant using robust and effective information (Davies et al., 2003).

For calculating a reliable fluid cube at the prospect location, and due to the fact that very limited well data was available on the OBC seismic survey (only Well-B, see Figure 9) we decided to generate a first fluid cube on the streamer seismic dataset. This survey contains better S/N ratio and has several wells that can be used to check the quality of the results. The definition of the wet trend is

expected to be therefore more reliable. The wet trend has been calculated using intercept and gradient values in an area located close to Well-A, at the same stratigraphic level where the prospect is located.

There, only shales and limited water-bearing silts are present. The resulting wet trend is rather well defined (**Figure 21a**) and enables the definition of the slope law (there, the fluid cube is defined by:  $R_0 + 0.345 \cdot G$ ).

The same exercise has been performed on the OBC seismic dataset (**Figure 21b**) and shows as expected a rather poorly defined background trend.

Since we do not foresee any major lithology or anisotropy changes within the KES target layer, we applied on the OBC intercept-gradient crossplot the same slope-law calculated on the streamer seismic dataset.

We then obtained a fluid cube for both seismic surveys.

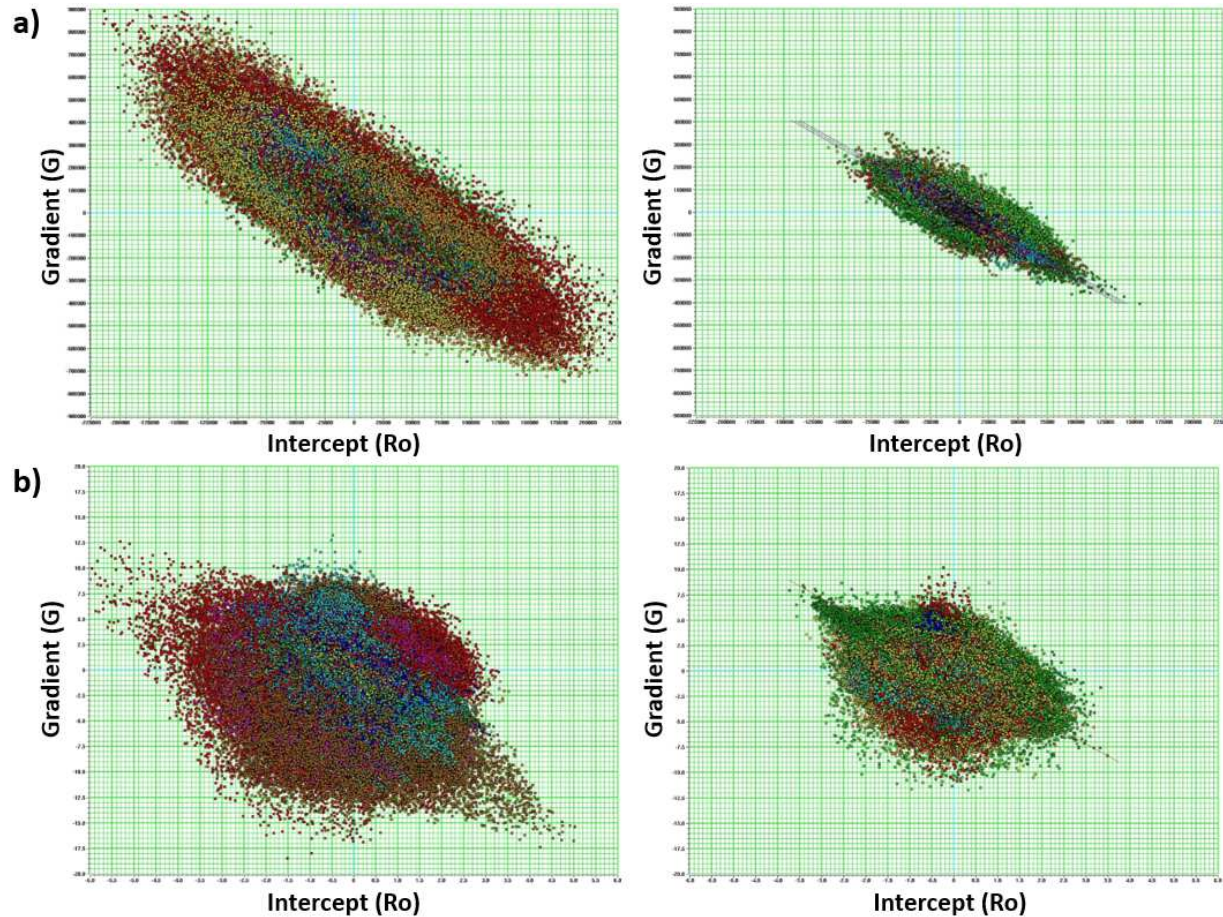


**Figure 21:** Fluid cube modelization over **a)** the streamer seismic survey and **b)** the OBC seismic dataset.

The left Intercept ( $R_0$ ) versus Gradient ( $G$ ) crossplots are including both brine and expected hydrocarbon-bearing zones, whereas the right crossplots are including only brine zones. We can observe that the streamer seismic dataset presents a far better wet-trend definition compared to the OBC seismic survey due to the low frequency content of the latter. Therefore, the decision was made to use the streamer data for defining the wet-trend.

A detailed QC has then been performed in order to validate these outputs. To do so, fluid cubes responses have been checked on all wells, on both seismic sections and interpreted horizons in order to validate gas responses at wells, as well as their lateral extensions. Some examples are presented on **Figure 22**. The observed results are perfectly in-line with the geological model detailed previously.

The fluid cube also enhanced - through additional analyses using both seismic sections and seismic amplitude maps - the definition of the DHI characteristics

of the assessed structure (**Figure 23**) and enabled a finer estimation of in-place volumes and associated uncertainties.

To estimate the Gross Rock Volume (GRV), we synthesized our understanding of the geological model using DHI characteristics. To do so, we used a combination of the top reservoir depth, thickness and coherency maps, as well as RMS seismic amplitude maps extracted from the fluid cube.

We then selected a lognormal GRV distribution adjusted on three GRV values (Reasonable Minimum, Median, and Reasonable Maximum) directly estimated from the Top reservoir depth map.



The reasonable minimum (P90) case has been limited to the small 4 way-dip structure at the top of the channel system (see **Figure 11a**), which corresponds to channel or proximal levee facies, limited to the West by the shale-plug of the terminal channel and by the spill-point of the 4-way dip in the other directions.

The median (P50) case is limited to the brightest seismic amplitude area at the top of the channel system along the channel axis (excluding shale plugs). It is interpreted as the best reservoir facies (amalgamated channels and proximal levees) and it excludes intermediate and distal levees.

The spill-point corresponds to the structural saddle present to the northern part of the complex and fits also with the disappearance of AVO effect to the North.

The reasonable maximum (P10) case corresponds to the maximum extent of the average RMS seismic amplitude anomaly calculated from the base to the top of the channel system (see **Figure 16d**). It is supposed to include most (but not all) the distal levees. But it also assumes that the Rosetta fault is sealing and that the entire channel is filled with gas. In addition, the maximum hydrocarbon column expected (200m) is far below what the pressure can retain and remains therefore a possible case.

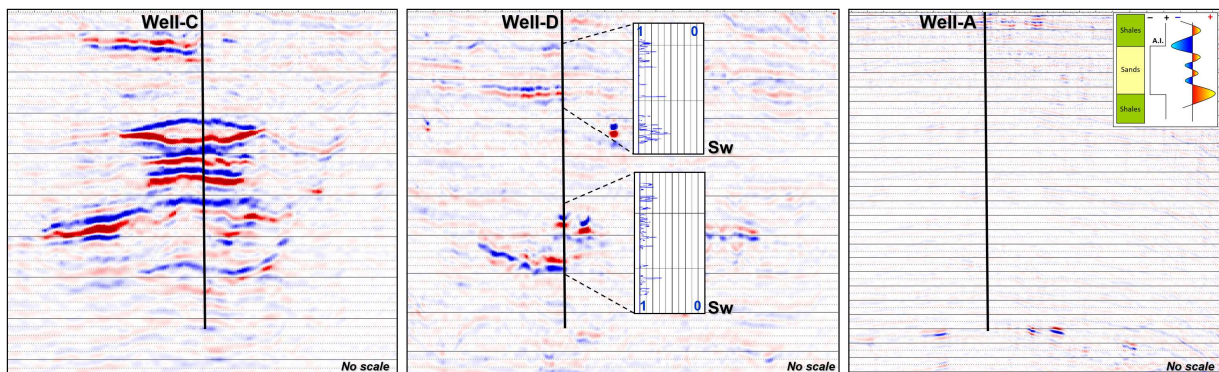


**Figure 22:** Quality control of fluid cube modelling on key wells.

The left seismic section highlights the fluid cube result over one of the wells of the Rosetta field. There, we can see that the well-known AVO effect of Well-C - characterised by high negative amplitude effect and a strong phase reversal - is nicely imaged. No fluid response is visible over Well-A presented on the right side of the figure.

This is indeed what we expected, as the well did not have any HC bearing reservoir over its entire section. We can see nevertheless some amplitude anomalies close to the bottom of the well. They are due to the high amplitude anhydrite patches that are present in the area at the Messinian level. The central figure presents the well-known limitation of AVO. There, Well-D shows some seismic amplitude anomalies reflecting the presence of gas shows but not in commercial quantities, as highlighted in the central figure by the displayed water saturation curves over the reservoir section.

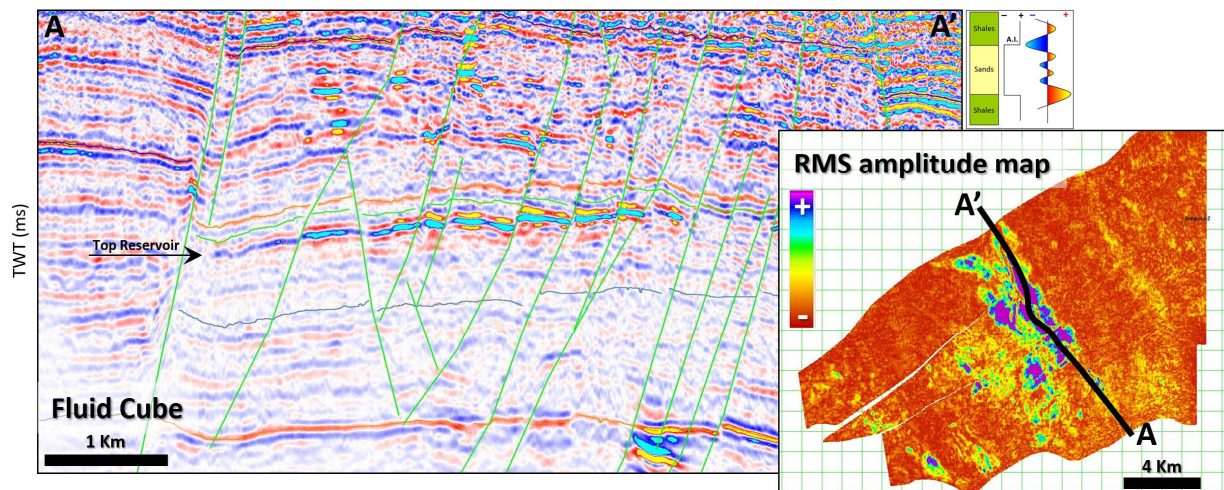


**Figure 23:** Reference fluid cube products through the studied prospect.

This full-stack seismic random line is extracted from the fluid cube. The line is longitudinal through the prospect channel axis. It must be compared with the ones (Full, Intercept and Gradient) presented on **Figure 17**. The map is an RMS seismic amplitude map extracted from Top to Bottom reservoir. It must be compared with the one presented on **Figure 16d** (Full-stack RMS amplitude).

In terms of pitfalls, according to [Firinu and Sahadic \(2014\)](#), the main reasons for failure of DHI supported prospects located in the Nile Delta are:

- Over-pressured sand or shale formations.
- Highly cemented sands.
- Low-porosity heterolytic sands.
- Coal beds and top of salt diapirs.
- Presence of anisotropy within the studied target interval.

Regarding our prospect, we do not expect unusual lithologies, such as coal or salt at target location, nor low porosity or cemented sands. Nevertheless, anisotropy or over-pressures cannot be ruled-out.

In addition, Low Saturation Gas (LSG) does not seem to be an issue in the region according to the well results versus the seismic amplitude characteristics database at our disposal, even if some nearby wells, such as Well-D (see [Figure 22](#)), are proven LSG reservoirs, but located in a different structural setting compared to our prospect location.

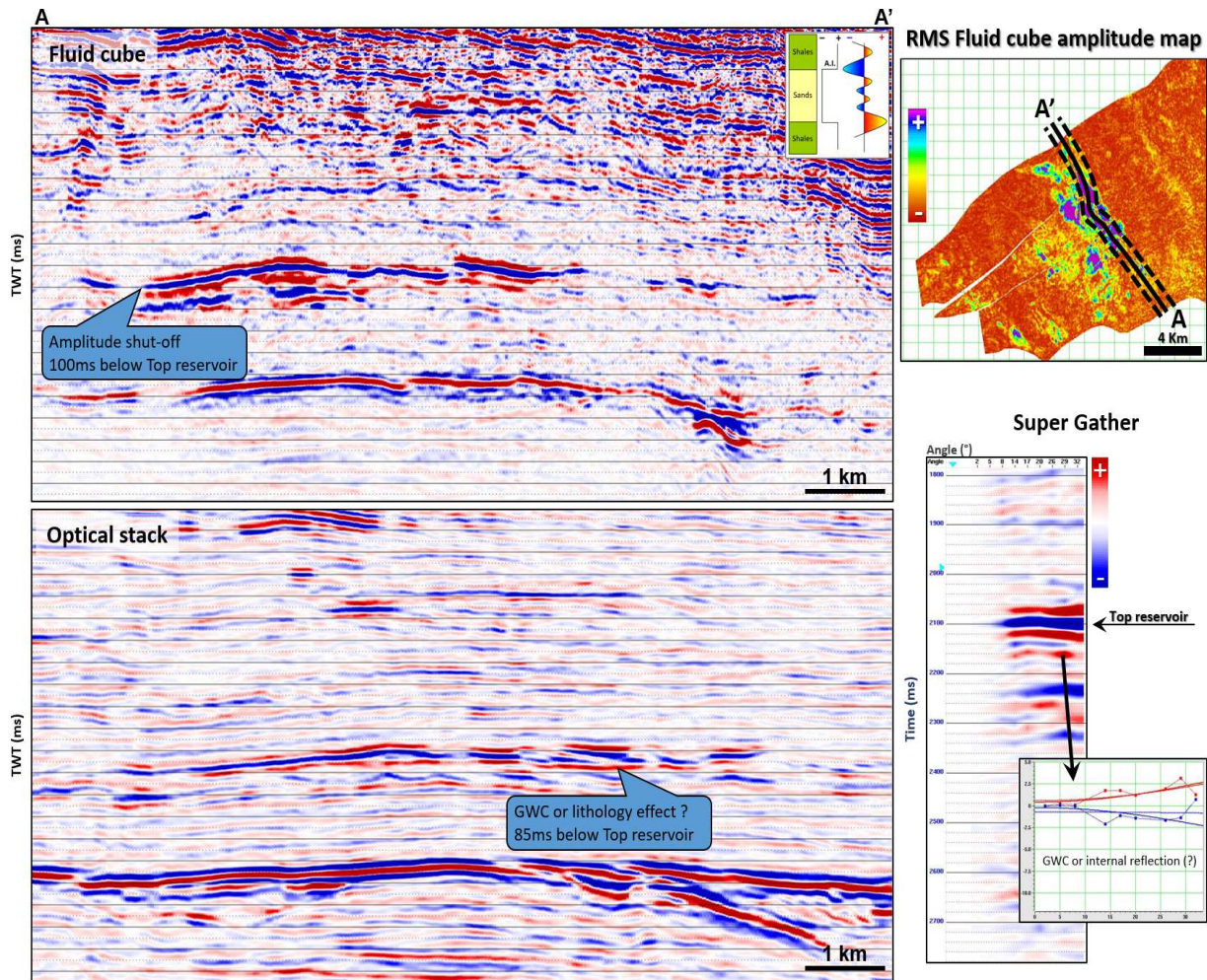


**Figure 24:** GWC hunting at prospect location.

This figure shows the three different approaches used for estimating the Gas Water Contact (GWC) at the prospect location using the fluid cube. The upper seismic section is a random line from the fluid cube going through the channel fairway axis, where we can notice near the southern (left) end, a sharp seismic amplitude shut-off located about 100ms below the Top reservoir, interpreted as a GWC.

The lower seismic section is an optical stack, consisting of 7 full-offset KPSTM seismic lines. The dashed lines on the RMS fluid cube amplitude map represent the limits of the data used in the optical stacking. We observe towards the northern part of the prospect a flat event located about 85ms below the Top reservoir. A possible second flat event, located on the central and southern part of the prospect can also be observed, about 70ms below the Top reservoir. A fault is separating those two flat events. If this flat event is a GWC, the fault should be therefore considered as sealing. Nevertheless, due to the high complexity of internal reflections within the amalgamated turbiditic channel complex, a lithology effect cannot be ruled out.

When going back to gathers (third approach), we can observe a strong positive reflector located at about 70ms below the Top reservoir, with a small AVO Class IIp effect. It may also reflect a fluid contact or highlight, as for the optical stacking, an internal reflector within the channel complex.

We also tried to determine the location of the Gas-Water-Contact (GWC) over the prospect using three different approaches illustrated in **Figure 24**.

To do so, we first analyzed the fluid cube amplitude response at the top reservoir. It is expected to show a strong negative seismic amplitude above GWC, and to be around zero below it. The fluid cube amplitudes are indeed dimming below the spill-point of the structure (**Figure 24**), which gives a GWC located at about 100ms below the top reservoir.

The second approach consists of generating an optical stack (i.e. a stack of parallel random lines defined along the channel axis). In our case, we use seven lines on each part of a central line going along a longitudinal orientation through the channel axis. The goal is to enhance flat events, such as GWC - which are indeed supposed to be at the same depth in all the seismic lines - while stacking-out lithologies. A flat event appears in the southern part of the channel (**Figure 24**), at about 85ms below the Top reservoir. It is important to keep in mind that the number of lines used to build the optical stack may be too limited to ensure a proper definition of the GWC. In term of potential additional limitations, the signal-to-noise (S/N) ratio of the OBC data may not be optimal, and the structural dips are low in the southern prospect area.

We finally analyzed the pre-stack CDP migrated gathers (see the super gather **Figure 24**). There, the top of the sands shows a strong negative reflector, becoming even more negative with the offset (i.e. Class III AVO as discussed earlier). But we observe a positive event located at 65 to 70ms below the top of the reservoir that may be interpreted as a GWC. However, this interpretation is very uncertain, as such a reflector can also be due to an internal reflection or an internal multiple.

Three potential GWC have thus been identified from data analysis, ranging from 65ms to 100ms below the top reservoir. Based on the AVO behavior of the of KES sands, we consider the GWC estimated from the fluid cube amplitudes as the most robust hypothesis.

The final summary regarding prospect DHI characteristics is presented in **Figure 25**. The strengths and weaknesses table highlights the DHI characteristics that have the most significant impact (both positive and negative) on the assessed prospect. The other tables give more details regarding the associated uncertainties for each DHI category.

We can notice that the major prospect strengths are the presence of a strong AVO effect, very different from the ones above, below and outside the reservoir at prospect location, as well as the fact that we did not observe any other anomalies that fit the expected geological model (indeed, two other leads are showing similar anomalies and are believed to be prospect analogues, see **Figure 15**). Regarding seismic amplitude and DHI characteristics, the main prospect weaknesses are the lack of a well-defined

seismic amplitude conformance at the downdip edge of the anomaly (edge effects), as well as additional pitfalls, main ones being the presence of a high porosity brine sand, an unexpected change in petro-elastic properties affecting the amplitude response, or the presence of overpressures (**Figure 25**).

### 5.3.3 Revised Pg assessment

A summary of the prospect assessment is shown on a spider chart (**Figure 26**) made-up of several graphs, each summarizing the analyses carried-out on each data quality component and DHI characteristics.

Following the detailed analysis of all the seismic amplitude and DHI characteristics over the prospect, we calculated a final DHI Index of 20%. If not weighted by the data quality index, the DHI Index would have been 27%. **Figure 27** presents an Initial Pg versus DHI Index graph showing the relative position of the assessed prospect in relation to the DHI Consortium's well database, where success and failure cases are highlighted.

With an Initial Pg of 19% and an uncalibrated DHI Index of 20%, we end up with a calibrated final Pg of 51% if we use the Bayesian method calibrated to the well results database. Using the DHI Consortium best fit graphical method, the final Pg is 75 % (the details of these calibration methods are currently confidential, as part of the DHI consortium). Whichever the calibration method used, this reflects a noticeable improvement of the Pg using the amplitude and DHI information.

The well was drilled following this evaluation and confirmed the presence of a 70m gas column at reservoir level, in-line with the optical stacking results. The seismic amplitude anomaly seen on the fluid cube confirmed to be mainly a gas effect rather than a lithological anomaly. The well results look consistent with the actual GWC depth of the northern part of the accumulation, where the trap shows a strong structural component. Everywhere else, the trapping mechanism is mainly stratigraphic, and the disappearance of the fluid cube anomaly is interpreted as a quick transition between the gas bearing sand reservoir and the lateral seal made of distal levees and/or marine shale.

Indeed, the lack of a direct link between the seismic anomaly and the 4-way closures defined on the top reservoir map confirms the fact that the presence of gas is not controlled by the structure but by stratigraphic elements (i.e. the presence of continuous or isolated sands).

Further studies based on logs data, such as FMI and dipmeter, as well as an additional well drilled on the western side of the constructive turbiditic channel-levees complex, also later confirmed the sedimentological depositional model.

Strengths and Weaknesses	Prospect Strengths		Prospect Weaknesses	
	***Excluding possible stacked pays, is the AVO effect anomalous compared to reflectors above and below?	AVO response of the target is distinctly different from that of reflectors above and below. (Grade 5)	***Downdip conformance (fit to structure) based on far-offset or stacked data	(...)
AVO observations using gathers, angle stacks, near-mid-far volumes, or windowed (gated) amplitudes	Strong negative reflection amplitude at NI with significant increase in reflection amplitude with offset. (Grade 5)	Lateral conformance based on far-offset or stacked data	(...)	
***Is the AVO effect anomalous compared to the same event outside the trap?	(...)	Hard streak above or within wet sands	(...)	
***Are unexplained anomalies seen on stacked or far offset data outside the target area (within same stratigraphic sequence) ?	(...)	Amplitude caused by sharp onset or increase in overpressure	(...)	
Amplitude change (as viewed on stacked P wave or far offset data)	(...)	Unexpected change in properties of the encapsulating shale (top or bottom) that affects the amplitude response	(...)	

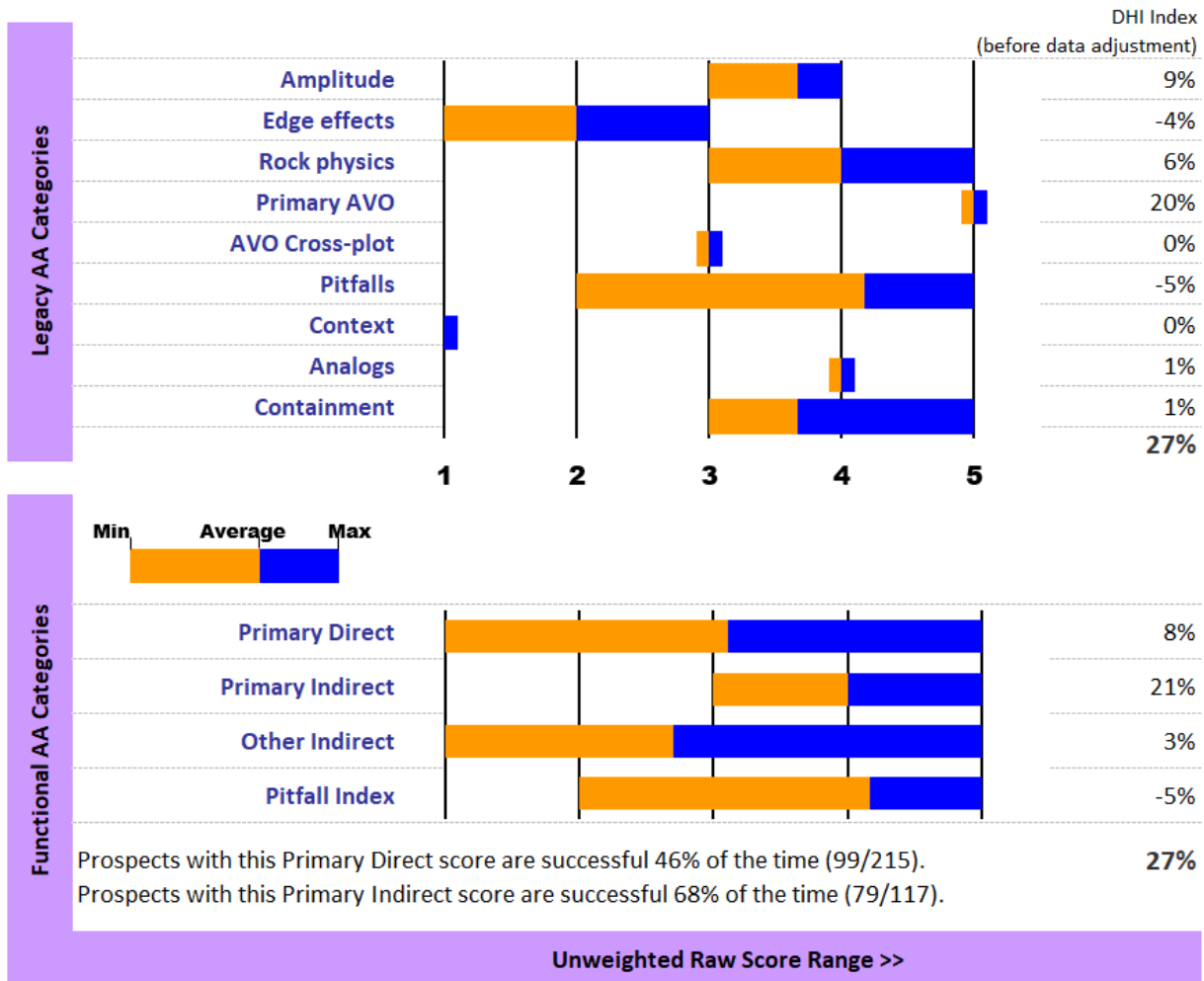


**Figure 25:** Prospect strengths and weaknesses and summarized DHI characteristics.

The upper table is a list of the assessed prospect's most significant DHI Characteristics, separated into strengths (left two columns) and weaknesses (right two columns). DHI characteristics that have proven to be the most statistically significant predictors of success or failure are flagged with 3 asterisks. Except for the first two entries, Grade Descriptors in the second and fourth columns have been removed due to confidentiality reasons.

The lower figure is a bar chart summarizing the raw grades assigned to all the DHI Characteristics over the assessed prospect, grouped by Legacy (top chart) and Functional (bottom chart) categories. For each category, a bar indicates the range of scores (i.e. minimum to maximum) given by the interpreter. The point where the bar changes from blue to orange is the average score for all the Characteristics in that category. The value column at the far right of the graph is the potential impact of the scores on the DHI Index before any Data Quality adjustment is applied.

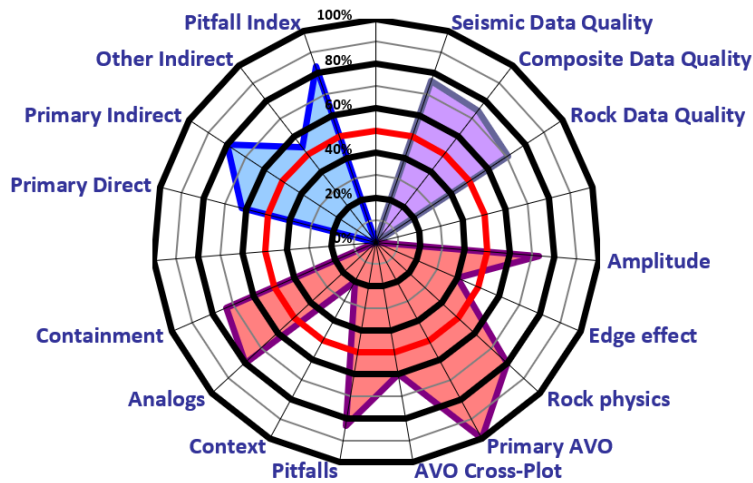


**Figure 26:** Spider summary diagram.

This spider plot represents the relative scoring values for key categories assessed during the prospect evaluation. Data Quality indicators are in purple and DHI Characteristics are shown organized by Legacy categories in red and then by Functional categories in blue. For all measurements, higher values (furthest from the center) are better.

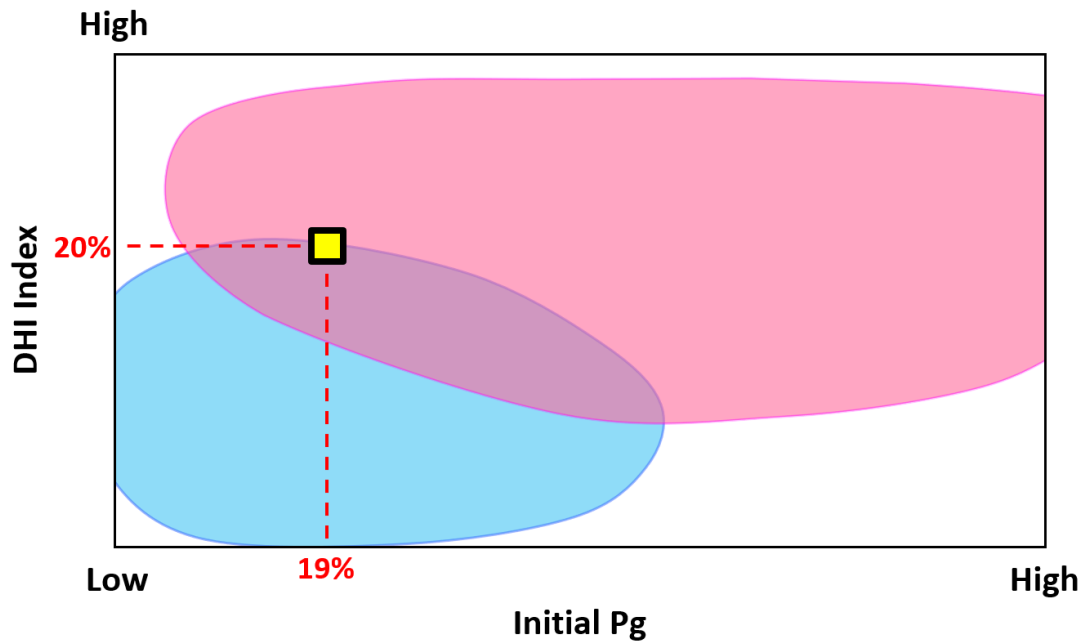


**Figure 27:** Initial Pg Vs. DHI Index.

The Initial Pg is on the horizontal axis, and the DHI Index (after data adjustment) is on the vertical axis. The prospects that were failures are represented by the blue area, while prospects that were discoveries are represented by the red area.

The assessed prospect is represented by a yellow square. This graph very quickly shows where the analyzed prospect lies in relation to the total discovery-failure statistics, which currently consists of about 350 previously drilled prospects with known outcomes. The exact location of the DHI Consortium failure and discovery wells have been removed from the graphic for obvious confidentiality reasons.

## 6. Conclusions

Each exploration team must efficiently incorporate seismic amplitude information into their risking and ranking schemes in order to obtain an unbiased portfolio, leading to enhanced exploration performance and meaningful exploration decisions. The Holy grail of risking is to provide an accurate estimate of the probability of finding commercial hydrocarbons among the company's prospect—inventory. When a prospect is amplitude-supported, as we can see in the Miocene to Pleistocene reservoirs of the Nile Delta area, this information must be incorporated into the risking and ranking schemes in the most efficient manner.

However, as indicated by [Fahmy and Reilly \(2006\)](#), no single attribute or technology is a universal remedy. The best results are obtained by both honoring the fundamentals of the geological assessment of Petroleum Systems, and by thorough integration of all DHI and associated G&G elements characterizing the assessed prospects.

A meaningful knowledge of the exploration context and experience are the key to success in a combined geological and geophysical approach to seismic amplitude risk assessment. Technical teams have to systematically collect and evaluate all available data. They must generate models and alternatives that are relevant to address the critical risks factors for enhanced prioritization using dedicated tools and workflows. The methodology and associated tools that have been detailed in this paper give a clear competitive advantage in the exploration game, thanks to a black box-free structure assessment, while avoiding overestimation of seismic amplitude and DHI effects.

Such an approach is easily adaptable to different geological environments, promotes integration between disciplines, and enables a straightforward process. This can lead to a systematic basis for a series of activities involved in oil and gas exploration, such as knowledge capitalization, target ranking through effective portfolio management, drilling planning, and eventually resource management.

## Acknowledgements

The authors would like to thank Chevron Petroleum Corporation for allowing the publication of this paper. We also express our gratitude to the former Engie EPI Egypt technical team for the relevant studies performed in order to highlight all the key aspects of the discussed case study, as well as the member companies of the DHI Consortium for providing key information to develop the Initial Pg and DHI Index methodologies.

We also thank Alexei Milkov from the Colorado School of Mines and Hermann Zeyen from Paris-Saclay University for their reviews and suggestions for improvements.

## References

Aal A., El Barkooky M., Gerrits H.J., Meyer M.S., Schander M., Zaki H., 2006: Tectonic evolution of the Eastern Mediterranean Basin and its significance for the hydrocarbon prospectivity of the Nile Delta deep-water area. *GeoArabia*, 6(3), pp.363-384.

Abd El-Hafez N., Abou-Mahmoud M., Mohamden M.I.I., 2014: Geological model delineation of sub-marine system channels in West Delta Deep Marine concession, Egypt. *Blue biotechnology*, 3, pp.523-534.

Ahmed N. El-Barkooky M., Helal M.A., 2002: Sequence Stratigraphy and Sedimentary History of the Neogene Nile Delta Major River Deltas of Africa: Compare and Contrast Hydrocarbon Systems, Cairo 2002: Ancient Oil-New Energy Technical Program.

Anwar A, Hassan S, Belhadj B, 2002: An integrated approach to determine hydrocarbon potential in low resistivity, thinly laminated reservoir: East-Delta area, Egypt. MOC 2002, Alexandria, Egypt, Abstract, 5p.

Avseth P., Mukerji T., Mavko G., 2011: Quantitative Seismic Interpretation. Applying Rock Physics Tools to Reduce Interpretation Risk. Cambridge University Press, 359p.

Baddeley M.C., Curtis A., Wood R., 2004: An Introduction to Prior Information Derived from Probabilistic Judgements: Elicitation of Knowledge, Cognitive Bias and Herding, vol. 239, Geological Society, London, Special Publications, pp. 15-27.

Baron J., Spranca M., 1997: Protected values. *Organizational Behavior and Human Decision Processes*, 70, pp.1-16.

Barsoum K., Aiolfi C., Dalla S., Kamal M., 1998: Evolution and hydrocarbon occurrence in the Plio-Pleistocene succession of the Egyptian Mediterranean Margin: Examples from the Nile Delta Basin. in M. Eloui, ed., *Proceedings of the 14th Petroleum Conference: Cairo, Egypt*, Egyptian General Petroleum Corporation, Vol. 1, pp 386-401.

Barsoum K, Della M, Kamal M, 2002: Gas chimneys in the Nile Delta slope and gas field occurrence. In: MOC 2002, Alexandria, Egypt, Abstract, 5p.

Bárdossy G., 2003: Geological reasoning and the problem of uncertainty. In *Modeling Geohazards: IAMG 2003 Proceedings*, Portsmouth UK; Editors J. Cubitt, J. Whalley, S. Henley. 5p.

Bentham P., 2011: Understanding crustal structure and the early opening history of the Eastern Mediterranean Basin, offshore Northern Egypt and the Levant. In: *New and emerging plays in the Eastern Mediterranean*, London, England, February 2011. The Geological Society of London, pp.67-68.

- Biju-Duval B., Montadert L., 1977: Structural history of the Mediterranean basins. Histoire structurale des bassins méditerranéens. Congrès, assemblée plénière de la commission internationale pour l'exploitation scientifique de la Méditerranée, symposium international, 25-29 octobre, 1976, Split, Yougoslavie, Ed. Technip.
- Boucher P.J., Dolson J.C., Siok J., Heppard P.D., 2004: Key challenges to realizing full potential in an emerging giant gas province: Nile Delta/Mediterranean Offshore, Deep Water, Egypt. Houston Geological Society, pp.25-27.
- Capen, 1976: The difficulty of assessing uncertainty: Journal of Petroleum Technology, v. 28/8, pp.843-850.
- Castagna J., Swan H., Foster D.J., 1998: Framework for AVO gradient and intercept interpretation. Geophysics, 63, pp.948-956.
- CCOP (Coordinating Committee for Offshore Prospecting in Asia), 2000. The CCOP Guidelines for Risk Assessment of Petroleum Prospects. [www.ccop.or.th/ppm/document/INWS1/INWS1DOC11\\_caluyong.pdf](http://www.ccop.or.th/ppm/document/INWS1/INWS1DOC11_caluyong.pdf).
- Citron G., Bond M., Carragher P., 2017: Exploration assurance team best practices: AAPG Search and Discovery article 70264, accessed December 15, 2018, [http://www.searchanddiscovery.com/pdfz/documents/2017/70264citron/ndx\\_citron.pdf.html](http://www.searchanddiscovery.com/pdfz/documents/2017/70264citron/ndx_citron.pdf.html).
- Citron G.P., Brown P.J., Mackay J., Carragher P., Cook D., 2018: The challenge of unbiased application of risk analysis towards future profitable exploration, in M. Bowman and B. Levell, eds., Petroleum geology of NW Europe: 50 years of learning: Proceedings of the 8th Petroleum Geology Conference, London, September 28–30, 2015, pp. 259-266.
- Connolly P., Wilkins S., Allen T., Schurter G., Rose-Innes N., 2005: Fluid and lithology identification using high-resolution 3D seismic data. In: Petroleum Geology: North-West Europe and Global Perspectives. Proceedings of the 6th Petroleum Geology Conference. Geological Society of London, A.G. Doré, B.A. Vining, Vol. 6.
- Cowan G., Shallow J., 1998: The Rosetta P1 field: a fast track development case study. In: Nile Delta Egypt. E.G.P.C. 14th exploration and production conference, vol 2, pp 222-235.
- Cozzi A., Cascone A., Bertelli L., Bertello F., Brandolese S., Minervini M., Ronchi P., Ruspi R., Harby H., 2017: Zohr Giant Gas Discovery - A Paradigm Shift in Nile Delta and East Mediterranean Exploration. Search and Discovery Article #20414, 22p.
- Cross N.E., Cunningham A., Cook R.J., Taha A., Esmia E., El Swidan N., 2009a: 3-D Seismic Geomorphology of a Deepwater Slope Channel System: The Sequoia Field, Offshore West Nile Delta, Egypt. Search and Discovery Article. Adapted from oral presentation at AAPG Convention, Denver, Colorado, June 7-10, 2009, 28p.
- Cross N.E., Cunningham A., Cook R.J., Taha A., Esmia E., El Swidan N., 2009b: Three-dimensional seismic geomorphology of a deep-water slope-channel system: The Sequoia field, offshore west Nile Delta, Egypt, AAPG Bulletin v. 93, p. 1063-1086.
- Davies D.J., Mcinalley A., Barclay F., 2003: Lithology and fluid prediction from amplitude versus offset (AVO) seismic data. Geofluids, 3(4), pp.219-232.
- De Bruin J.A., 2020: Domains and trends in AVO. First Break, February 2020, 38(2), pp.29-36.
- Deibis S., Futyan A.R., Ince D.M., Morley R.J., Seymour W.P., Thompson S., 1986: Stratigraphic framework of the Nile Delta and its implications with respect to regions, hydrocarbon potential. E.G.P.C. 8th exploration conf., Abstract, 5p.
- Demaison G., Huizinga B.J., 1994: Genetic classification of petroleum systems using three factors: charge, migration, and entrapment, in L.B. Magoon and W.G. Dow, eds., The Petroleum System--From Source to Trap: AAPG Memoir 60, p. 73-89
- Dolson J.C., Boucher P.J., Teasdale J., Romine K., 2002: Basement Structural Controls on Sedimentation and Hydrocarbon Charge, Nile Delta, Egypt, in Nile Delta Petroleum Systems and Exploration Potential, CAIRO 2002: Ancient Oil-New Energy Technical Program.
- Dolson J.C., 2020: The Petroleum Geology of Egypt and History of Exploration. Springer Nature Switzerland, Z.Hamimi et al. (eds.), The Geology of Egypt, Regional Geology Reviews, pp.635-658.
- Duff B.A., Hall D.M., 1996: A model-based approach to evaluation of exploration opportunities. In Doré A.G. and Sindling L. (Ed.), Quantification and Prediction of Petroleum Resources, Special Publication 6, NPF, pp.183-198.
- Elewa A., Alfay M., Hemdan K., Salem A., 2002: Potential gas reserves with Pliocene North Port Said Concession, Egypt. Proceeding in international Exhibition and Conference for gas industry in Middle East and North Africa, Intergas Conference 2002, Egypt, pp. 45-56.
- El-Heiny I., 1982: Neogene stratigraphy of Egypt, Newsletter Stratigraphy, 11 (2), p.41-54.
- El Maghraby, F., Rizk, A., Hussien, M., 2010: Seismic capability of finding gas and oil on the onshore Nile Delta of Egypt, MOC 2010, Alex., Egypt. Abstract, 5p.
- Esestime P., Hewitt A., Hodgson N., 2016: Zohr – A newborn carbonate play in the Levantine Basin, East-Mediterranean. First Break, Feb. 2016, 34, pp.87-91.

- Fahmy W.A., Reilly J.M., 2006: Applying DHI/AVO Best Practices to Successfully Identify Key Risks Associated with a Fizz-water Direct Hydrocarbon Indicator in the Norwegian Sea. SEG abstracts, pp.553-556.
- Feng H., Bancroft J.C., 2006: AVO principles, processing and inversion. CREWES Research Report, Vol.18 (2006), 19p.
- Fervari M., Luoni F., 2006: Quantitative characterization of seismic thin beds: a methodological contribution using conventional amplitude and seismic inversion. *First Break*, 24, pp.53-62.
- Finlayson A., 2018: Prospect Maturation and Post Well Look Backs; Sharing good practices. Oil and Gas UK Exploration Conference 2018, Abstract, 5p.
- Fischhoff B., Slovic P., Lichtenstein S., 1977: Knowing with certainty: the appropriateness of extreme confidence. *Journal Exp. Psychol. Hum. Percept. Perform.* 3, pp.552-564.
- Firinu M, Sahadic S (2014) Understanding formation anisotropy within a false bright spot Anomaly response. [http://www.euromedoffshore.com/files/2012\\_Presentations/MauroFirinu.pdf](http://www.euromedoffshore.com/files/2012_Presentations/MauroFirinu.pdf).
- Ffrench J., 2020a: The Tamar Gas Field - A Triplet of Tuning Rings. LinkedIn publication: <https://www.linkedin.com/pulse/tamar-gas-field-triplet-tuning-rings-jon-ffrench/>. Adapted from Needham et al., 2010 in AAPG Memoir 113, Giant Oil & Gas Fields of the Decade 2000-2010, 13.
- Ffrench J., 2020b: Constructive Adjacent Tuning Ring - Balsam Field, Egypt. LinkedIn publication: <https://www.linkedin.com/pulse/constructive-adjacent-tuning-ring-balsam-field-egypt-jon-ffrench/>. Adapted from Dana Gas Analyst online presentations 2015/16, Balsam Field, onshore Nile Delta, Egypt.
- Ffrench J., 2020c: Hawkeye Prospect Tuning Rings - Palawan, Philippines. LinkedIn publication: <https://www.linkedin.com/pulse/hawkeye-prospect-tuning-rings-palawan-philippines-jon-ffrench/>.
- Forrest M., 2010: Learning from 40 Years' Experience: Risking Seismic Amplitude Anomaly Prospects. AAPG Annual Convention, New Orleans, Louisiana, April 11-14, 2010, 29p.
- Forrest M., R. Roden, Holeywell R., 2010: Risking seismic amplitude anomaly prospects based on database trends, *The Leading Edge*, 29, pp.570-574.
- Fournier A., Mosegaard K., Omre H., Sambridge M., Tenorio L., 2013: Assessing uncertainty in geophysical problems - Introduction. *Geophysics*, Vol. 78, No. 3 (May-June 2013); p. WB1-WB2.
- Fraser A.J., 2011: A regional overview of the exploration potential of the Middle East: a case study in the application of play fairway risk mapping techniques. Geological Society, London, Petroleum Geology Conference series, 7, pp.791-800.
- Galbiati M., Fervari M., Cavanna G., 2009: Seismic evaluation of reservoir quality and gas reserves of DHI-supported deep water systems in the offshore Nile Delta. *First Break*, 27(2), 5p.
- Geng Z., Wang H., Fan M., Nie Z., Ding Y., Chen M., 2019: Predicting seismic-based risk of lost circulation using machine learning. *Journal of Petroleum Science and Engineering*, 176, pp.679-688.
- Glover P.W.J., Hole M.J., Pous J., 2000: A modified Archie's law for two conducting phases. *Earth and Planetary Science Letters*, 180(3-4), pp.369-383.
- Glover P.W.J., 2015: Geophysical properties of the near surface earth: Electrical properties. In: *Treatise on Geophysics*, Elsevier, pp.89-137.
- Gong C., Wang Y., Zhu W., Li W., Xu Q., 2013: Upper Miocene to Quaternary unidirectionally migrating deep-water channels in the Pearl River Mouth Basin, northern South China Sea. *AAPG Bull.*, 97, pp.285-308.
- Gotautas V.A., 1963: Quantitative Analysis of Prospect to Determine Whether it is Drillable. *AAPG Bulletin* (1963), 47(10), pp.1794-1812.
- Granado P., Urgeles R., Sàbat F., Albert-Villanueva E., Roca E., Anton Muñoz J., Mazzuca N., Roberto G., 2016: Geodynamical framework and hydrocarbon plays of a salt giant: the NW Mediterranean Basin. *Petroleum Geoscience*, August 2016, 22, pp.309-321.
- Haffinger P., von Wussow P., Doulgeris P., Henke C., Gisolf A., 2015: Reservoir Delineation by Applying a Nonlinear AVO Technique - A Case Study in the Nile Delta. 77th EAGE Conference & Exhibition 2015, IFEMA Madrid, Spain, 1-4 June 2015, Abstract, 5p.
- Hamimi Z., El-Barkooky A., Martines Frias J., Fritz H., Abd El-Rahman Y., 2020: The geology of Egypt. *Regional geology reviews*, Springer Nature Switzerland, 710p.
- Hanafy S., Nimmagadda S., Sharaf Eldin S., Hemdan K., Farhood K., Mabrouk W., 2014: New insights on interpretation of seismic attributes in Nile-Delta basins for analyzing Pliocene geological characteristics. *MOC 2014*, Alexandria, Egypt, Abstract, 5p.
- Hanafy S., Farhood K., Mahmoud S.E., Nimmagadda S., Mabrouk W.M., 2018: Geological and geophysical analyses of the different reasons for DHI failure case in the Nile Delta Pliocene section. *Journal of Petroleum Exploration and Production Technology*, Springer, 13p.



- Harms J.C., Wray J.L., 1990: Nile Delta. In: *The Geology of Egypt*. A.A. Balkema / Rotterdam / Brookfield, 17, pp.329-343.
- Harwood C., Hodgson N., Ayyad M., 1998: The application of sequence stratigraphy in the exploration for the Plio-Pleistocene hydrocarbons in the Nile Delta. EGPC 14th Petroleum Conference, 2, pp.1-13.
- Hashem A., Rizk R., Gaber M., Bunt R., Mckeen R., 2010: Petroleum system analysis of south east El Mansoura area and its implication for Hydrocarbon exploration, onshore Nile Delta, Egypt, MOC 2010, Alex., Egypt. Abstract, 5p.
- Helmy M., Fouad O., 1994: Prospectivity and play assessment of Abu Qir area, Nile Delta, Egypt. In: *E.G.P.C. 12th exploration and production conference*, 1, pp.277-292
- Hesthammer, J., Stefatos, A., Boulaenko, M., Vereshagin, A., Gelting, P., Wedberg, T., and Maxwell, G., 2010: CSEM technology as a value driver for hydrocarbon exploration. *Marine and Petroleum Geology*. Volume 27, Issue 9, October, pp.1872-1884.
- Holtz M.H., 2002: Residual Gas Saturation to Aquifer Influx: A Calculation Method for 3-D Computer Reservoir Model Construction. *SPE Proceedings - Gas Technology Symposium*. 10.2118/75502-MS, 10p.
- Houck R.T., 1999: Estimating uncertainty in interpreting seismic indicators. *The Leading Edge*, 18 (3), pp.320-325.
- Houck R.T., 2002: Quantifying the uncertainty in an AVO interpretation. *Geophysics*, 67, 1, p.117-125.
- Ibrahim M., Gaafar G.R., Esmail E., Hassan A., 2010: Hydrocarbon exploration in a Tertiary stratigraphy of the offshore Nile Delta Basin, Egypt. *Petroleum Geology Conference and Exhibition 2010*, Geological Society of Malaysia. 29-30<sup>th</sup> March 2010, Kuala Lumpur Convention Center, Kuala Lumpur, Malaysia, 4 p.
- Jeng, 2006: A selected history of expectation bias in physics. *American Journal of Physics*. 74 (7), pp.578-583.
- Johns D.R., Squire S.G., Ryan M.J., 1998: Measuring exploration performance and improving exploration predictions - with examples from Santos's exploration program 1993-96. *APPEA J.* 38, pp.559-569.
- Kahneman, D., Tversky A., 1979: Prospect theory: An analysis of decisions under risk: *Econometrica*, v. 47/2, p. 263-292.
- Kellner A., Brink G.J., Khawaga H.E., 2018: Depositional history of the western Nile Delta, Egypt: Late Rupellian to Pleistocene. *Am. Assoc. Pet. Geol. Bull.* 102, pp.1841-1865.
- Khalid P., Qayyum F., Broseta D., 2010: Low Gas-saturation effect on AVO response. *PAPG/SPE Annual Technical Conference*, November 10-11 2010, Islamabad, pp.125-136.
- Kunjan, B., 2016: Exploration Chance of Success Predictions - Statistical Concepts and Realities. *ASEG-PESA- AIG 2016 August 21-24*, Adelaide, Australia. Abstract, 5p.
- Laver R., Randen T., Warner S., 2012: How geoscience decisions support software tools have evolved and what it means for E&P companies: *First Break*, v. 30, pp. 121-126.
- Lecerf D., Barros C., Hodges E., Valenciano A., Chemingui N., Lu S., Johann P., Thedy E., 2017: Sparse seabed seismic acquisition for 3D/4D reservoir imaging using high-order multiples. Application to Jubarte PRM. *SBGf and EXPOGEF Expanded Abstracts*, pp.1742-1745.
- Leila M., Moscariello A., Kora M., Mohamed A., E., 2020: Sedimentology and reservoir quality of a Messinian mixed siliciclastic-carbonate succession, onshore Nile Delta, Egypt. *Marine and Petroleum Geology*, Vol. 112, February 2020, 19p.
- Long A., 2019: What Does 'Sparse' Really Mean Anyway? Ocean Bottom Nodes, Towed Streamers and Imaging. LinkedIn publication. <https://www.linkedin.com/pulse/what-does-sparse-really-mean-anyway-ocean-bottom-nodes-andrew-long/>.
- Longley I., Brown J., 2016: Why bother ? (with play-based exploration): the five reasons why play based exploration worthwhile in a modern busy understaffed and overworked exploration company environment. *Search and Discovery article #110227*, adapted from AAPG SEG conference and exhibition, Melbourne, Australia, September 13-16, 2015, 97p.
- Maguire D., Seligmann P., El Fattah A., 2009: Lithology Classification and Prediction in the Abu Sir Field, Nile Delta, Offshore Egypt. *SEG Houston 2009 International Exposition and Annual Meeting, Technical Program Expanded Abstracts*, 4p.
- Magoon L.B., 1988: The petroleum system - a classification scheme for research, exploration, and resource assessment, in L.B.
- Magoon L.B., Dow W.G., 1994: The petroleum system, in L.B. Magoon and W.G. Dow, eds., *The Petroleum System--From Source to Trap*: AAPG Memoir 60, p. 3-24.
- Maver K.G., 2019a: The Hydrocarbon Pre-Drill Prediction Toolbox - How sharp are the technologies in the hydrocarbon pre-drill prediction toolbox for calculating the Geological Chance for Success (GCOS) in oil and gas exploration ? *GeoExpro*, Vol. 16, No. 1.
- Maver K.G., 2019b: Review of statistical probabilities from technologies used for pre-drill hydrocarbon prediction. Abstract submitted to EAGE, London, 5p.

- Merkhofer M.W., 1987: Quantifying judgmental uncertainty: Methodology, experiences, and insights. *IEEE Transactions on Systems, Man, & Cybernetics*, 17(5), pp.741-752.
- Milkov A., 2015: Risk tables for less biased and more consistent estimation of probability of geological success (PoS) for segments with conventional oil and gas prospective resources. *Earth Science Reviews*, pp.453-476.
- Milkov A.V., 2017: Integrate instead of ignoring: Base rate neglect as a common fallacy of petroleum explorers. *AAPG Bulletin*, 101 (12), pp.1905-1916.
- Milkov A.V., Samis J.M., 2020: Turning dry holes from disasters to exploration wisdom: Decision tree to determine the key failure mode for segments in conventional petroleum prospects. *AAPG Bulletin*, 104 (2), February 2020, pp. 449-475.
- Moktar M., Saad M., Selim S., 2016: Reservoir architecture of deep marine slope channel, Scarab field, offshore Nile Delta, Egypt: Application of reservoir characterization. 25 (4), Dec. 2016, pp.495-508.
- Monir M., Shenkar O., 2016: Pre-Messinian petroleum systems and trap style in the offshore Western of Nile Delta; an integrated geological and geophysical approach. *Africa energy and Technology Conference*, 5-7 December 2016, Abstract, 7p.
- Nabawy B., Basal A., Sarhan M., Safa M., 2018: Reservoir zonation, rock typing and compartmentalization of the Tortonian-Serravallian sequence, Tamsah Gas Field, offshore Nile Delta, Egypt. *Petroleum Geology*, 92, pp. 609-631.
- Nashaat M., Sallam Y., Elsherif A., 2001: Utilizing magnetic resonance logging for improved formation evaluation in the Mediterranean thinly laminated gas bearing formations: a case study. *SPE Annual Technical Conference and Exhibition*, New Orleans, Louisiana, pp 1-14.
- Needham D.L., Pettingill H.S., Christensen C.J., Ffrench J., Karcz W., 2017: The Tamar Giant Gas Field: Opening the Subsalt Miocene Gas Play in the Levant Basin. In R. K. Merrill and C. A. Sternbach, eds., *Giant Fields of the Decade 2000–2010: AAPG Memoir 113*, pp. 221-256.
- Nixon S., Hallam T., Constantine A., 2018: Ranking DHI attributes for effective prospect risk assessment applied to the Otway Basin, Australia. *Australian Exploration Geoscience Conference*, Abstract, 5p.
- O'Brien J., 2004: Seismic amplitudes from low gas saturation sands. *The Leading Edge*, 23(12), pp.1209-1320.
- O'Brien J., 2005: Seismic Amplitude Anomalies associated with Low Gas Saturation Sands A Case Study from Green Canyon Block 473 in the Gulf of Mexico. *Conference Proceedings, 67th EAGE Conference & Exhibition*, Jun 2005, cp-140-00043. 5p.
- Olofsson B., Mitchell P., Doychev R., 2012: Decimation test on an ocean-bottom node survey: Feasibility to acquire sparse but full-azimuth data. *The Leading Edge*, 31(4), pp.457-464.
- Oswald M.E., Grosjean S., 2004: Confirmation bias. In: Pohl, R.F. (Ed.), *Cognitive Illusions: A Handbook on Fallacies and Biases in Thinking, Judgement and Memory Psychology*, Press, Hove, UK, pp.79-96.
- Peel, F. J. and Brooks J. R. V., 2015a: What to expect when you are prospecting: How new information changes our estimate of the chance of success of a prospect. *AAPG Bulletin*, v. 99, no. 12 (December), p. 2159–2171.
- Peel, F. J. and White, J. 2015b: Do technical studies reduce subsurface risk in hydrocarbon exploration: and if not, how do they add value ? Bowman, M., Smyth, H. R., Good, T. R.,
- Peel F. J. and Brooks J. R. V., 2016: A practical guide to the use of success versus failure statistics in the estimation of prospect risk. *AAPG Bulletin*, v. 100, no. 2 (February), p. 137–150.
- Pervez K., Farrukh Q., Broseta, D., 2010: Low Gas-Saturation Effect on AVO Response. *PAPG/SPE Annual Technical Conference*, November 10-11, 2010, Islamabad, pp.125-136.
- Pettingill H.S., Holeywell R., Forrest M., Roden R., Weimerand P., Faroppa J., 2019: DHIs and Flat Spots: the Miocene Levant basin within a global perspective. 2019 *AAPG Geoscience Technology Workshop*, Tel Aviv, Israel, Feb. 2019, pp.26-27.
- Phelps D., Bedingfield J., Bork J., Allard D., Dodd T., 2003: Characteristics of Recent Oil and Gas Discoveries in the Deep-Water Portion of the Western Nile Delta, Egypt. *Abstract, Houston Geological Society Bulletin*, Volume 45, No. 10, June 2003, pp.13-15.
- Prinzhofer A., Deville E., 2013: Origins of hydrocarbon gas seeping out from offshore mud volcanoes in the Nile delta. *Tectonophysics*, Volume 591, pp.52-61.
- Rashid A., El-Gharabawy S., Abou Shagar, S., 2018: Geological and Structural Evaluation on Tamsah Gas Field, NE-offshore Nile Delta, Egypt. *International Journal of Scientific Engineering and Applied Science (IJEAS) – Volume-4, Issue-7, July 2018*, pp.18-29.
- Rio D., Raffi I., Villa G., 1990: Pliocene-Pleistocene calcareous nannofossil distribution patterns in the

- western Mediterranean. Proceedings of the Ocean Drilling Program, pp. 513-533.
- Rizzini, A., Vezzani, F., Coccocetta, V., Milad, G., 1978: Stratigraphy and sedimentation of Neogene-Quaternary section in the Nile delta area, (A.R.E). *Mar. Geol.* 27, pp.327-348.
- Roden R., Forrest M., Holeywell R., 2005: The impact of seismic amplitudes on prospect risk analysis, *The Leading Edge*, 24, pp.706-711.
- Roden R., Forrest M., Holeywell R., 2012: Relating seismic interpretation to reserve/resource calculations: Insights from a DHI consortium. *The Leading Edge*. September 2012. Special section: Geophysics in Reserves Estimations. pp.1066-1074.
- Roden R., Forrest M., Holeywell R., Carrand M., Alexander P., 2014: The role of AVO in prospect risk assessment. *Interpretation*, 2, SC61-SC76.
- Rose P.R., 1987: Dealing with risk and uncertainty in exploration: How can we improve ? *AAPG Bulletin*, v.71, nb.1, pp.1-16.
- Rose P.R., 1992: Chance of success and its use in petroleum exploration. In: Steinmetz, R. ed., *The Business of Petroleum Exploration*. AAPG Treatise of Petroleum Geology - Handbook of Petroleum Exploration, Chapter 7, pp.71-86.
- Rose P.R., 2001a. Prospect should be portfolio fit. *AAPG Explorer* 8.
- Rose P.R., 2001b: Risk Analysis and Management of Petroleum Exploration Ventures. *AAPG Method in Exploration*, 12, 60p.
- Rose P.R., 2004: Risk Analysis and Management of Petroleum Exploration Ventures. *AAPG methods in Exploration series*, No. 12, 164p.
- Rose P.R., 2017: Evolution of E & P Risk Analysis (1960-2017). *AAPG 100th Annual Convention and Exhibition*, Houston, Texas, April 2-5, 2017. 45p.
- Rose P.R., Citron G.P., 2000: The Prospector Myth vs. Systematic Management of Exploration. *Portfolios: Dealing With the Dilemma*. Houston Geological Society Bulletin, October 2000.
- Rudolph K.W., Goulding F.J., 2017: Benchmarking Exploration Predictions and Performance Using 20+ Years of Drilling Results: One Company's Experience. *AAPG Bulletin*, v. 101, no. 2 (February 2017), pp. 161-176.
- Rühl T., Samuelsson J., 2017: Multi-attribute Bayesian risk modification - a case study from the Norwegian Barents Sea. *First Break*, 35, pp.51-58.
- Rutherford S.R., Williams R.H., 1989: Amplitude-versus-offset variations in gas sands: *Geophysics*, 54, pp.680-688.
- Samuel A., Kneller B., Raslan S., Sharp A., Parsons C., 2003: Prolific deep-marine slope channels of the Nile Delta, *Egypt. AAPG bulletin*, 87 (4), April 2003, pp 541-560.
- Said R., 1990: *The geology of Egypt vol 1*. A.A. Balkema Publishers, Rotterdam, The Netherlands, 734p.
- Said R., 1981: *The geological evolution of the River Nile*. Springer-Verlag, 151 p.
- Sansal, 2014: Contribution of Seismic Amplitude Anomaly Information in Prospect Risk Analysis. Univ. Houston Master Thesis. 43p.
- Sarhan M., Barsoum K., Bertello F., Talaat M., Nobili M., 1996: The Pliocene play in Mediterranean offshore, structural setting and growth faults-controlled hydrocarbon accumulations in the Nile Delta basin. A comparison with Niger Delta basin. *E.G.P.C. 13th exploration and production conference*, Abstract, 5p.
- Schumacher D., 2012: Hydrocarbon Microseepage - A Significant but Underutilized Geologic Principle with Broad Applications for Oil/Gas Exploration and Production. Adapted from poster presentation at AAPG Annual Convention and Exhibition, Long Beach, California, April 22-25.
- Shaaban F., Lutz R., Littke R., Bueker C., Odisho K., 2006: Source-Rock evaluation and basin modeling in NE Egypt (NE Nile Delta and Northern Sinai). *Journal of Petroleum Geology*, 29(2), April 2006, pp.103-124.
- Sharaf E., Korrat I., Seisa H., Esmail E., 2014: Seismic Imaging and Reservoir Architecture of Sub-Marine Channel Systems Offshore West Nile Delta of Egypt. *Open Journal of Geology*, 2014, 4, pp.718-735.
- Simm R., 2017: A 'sense check' method for incorporating seismic amplitude information into prospect risk. *First Break*, pp.45-49.
- Simm R., 2020: DHI scenarios in exploration: a personal view. *First Break*, February 2020, 38(2), pp.37-42.
- Simm R., Bacon, 2014: *Seismic Amplitudes*, Cambridge University Press, 271p.
- Smalley P.C., Begg S.H., Naylo M., Johnsen S., Godi A., 2008: Handling risk and uncertainty in petroleum exploration and asset management: an overview. *AAPG (Am. Assoc. Pet. Geol.) Bull.*, 92 (10) (2008), pp.1251-1261.
- Snow J.H., Dore A.G., Dorn-Lopez D.W., 1996: Risk analysis and full-cycle probabilistic modelling of prospects: a prototype system developed for the Norwegian shelf. In: Dore A.G., Sinding-Larsen R. Eds., *Quantification and Prediction of Petroleum Resources*, Norwegian Petroleum

Society (NPF), Special Publication 6, Elsevier, Amsterdam, pp. 153-165.

Stabell C., Lunn S., Breirem K., 2003: Making effective use of a DFI: A practical Bayesian approach to Risking Prospects. SPE 82020.

Stirling E.J., 2003: Architecture of fluvio-deltaic sandbodies: the Namurian of Co. Clare, Ireland, as an analogue for Plio-Pleistocene of the Nile Delta. University of Leeds, PhD thesis, 357p.

Syed M., 2015: Black box thinking: Why most people never learn from their mistakes -but some do: New York, Portfolio/Penguin, 325 p.

Sykes M.A., Hood K.C., Salzman S.N., Vanderwater C.J., 2011: "Say what we mean and mean what we say": The unified risk model as a force for shared understanding (abs.): AAPG International Conference and Exhibition, Milan, Italy, October 23–26, 2011, <http://www.searchanddiscovery.com/abstracts/html/2011/ice/abstracts/abstracts410.html>.

Tawadros E., 2011: Geology of North Africa. CRC Press, Taylor and Francis Group, 931p.

Tversky A., Kahneman D., 1974: Judgment under uncertainty: Heuristic and biases: Science, New Series, v. 185/4157. pp.1124-1131.

Watson P., 1998: A process for estimating geological risk of petroleum exploration prospects. APPEA J. 34, pp.577-583.

Westwood Group, 2019: The impact of DHIs on exploration performance. Westwood Global Energy Group. Wildcat. Internal publication. 29p.

Westwood Group, 2020: Improved exploration success rates for DHI supported wells. Westwood Global Energy Group. Wildcat. Internal publication. 29p.

Whaley J., 2008: The Raven field, planning for success. GeoExPro, Feb. 2008, pp.36-40.

White D.A., 1993: Geologic risking guide for prospects and plays. AAPG bulletin, 77 (12), pp.2048-2064.

Wigger S., Simpson M., Nada H., Larsen M., Haddag M., 1996: Ha'py field: the result of Pliocene exploration in the Ras el Barr concession, Nile Delta. Proceedings of the 13rd EGPC Petroleum Conference, Cairo, Egypt, 1 (exploration), pp.181-192.

Wojcik K.M., Esepou I.S., Kalejaiye A.M., Umahi O.K., 2016: Bright spots, dim spots: Geologic controls of direct hydrocarbon indicator type, magnitude and detectability, Niger Delta Basin. Interpretation, 4(3), SN45-SN69.

Zach J.J., Frenkel M.A., Ostvedt-Ghazi A.M., de Lugao P., Ridyard D., 2009: Marine CSEM methods for 3D hydrocarbon field mapping and monitoring. Abstract. 11th International Congress of the Brazilian Geophysical Society, Salvador, Brazil, August 24-28, 2009. 6p.

Zaghoul Z.M., El Gamal M.M., Shaaban F.F., Yousef A.F., 2001: Plates interactions and petroleum potentials in the Nile Delta, Modern and Ancient. Cairo, pp.41-53.